CO_2 CAPTURE FROM FLUE GAS IN A MICRO-STRUCTURED BED

Final Report

Presented to

Alberta Innovates: Energy and Environment Solutions

Attn: Dr. Duke du Plessis

Abdelhamid Sayari[1] and Wei Liu[2]

(1) Department of Chemistry, University of Ottawa, Ottawa ON K1N 6N5, Canada

(2) Pacific Northwest National Laboratory, PO Box 999, Richland, WA 99352

May, 2013

EXECUTIVE SUMMARY

- Funding was made available to the University of Ottawa's team on May 2, 2012
- It took several weeks to establish a subcontract with PNNL (different formats, different pr^{oc}edures, discussions of some points, etc)
- The first installment was sent to PNNL on June 28, 2012, and the project started at PNNL on July 28.
- Nonetheless, for reporting purposes, we assume that the project has officially started on May 1, 2012.
- The following is the adjusted timetable and the status of each milestone.

Milestones	MAY	JUNE	JULY	AUG	SEPT	OCT	NOV	DEC	JAN	FEB	MAR	APR	Status
1	Project setup/ Hiring												achieved
2		Lab-scale synthesis											achieved
3				Scale-up synthesis									achieved
4			Characterization CO2 adsorption measurements/Stability										achieved
5				Fabrication of structured bed									achieved
6						Progress report							achieved
7							Debugging Testing						achieved
8							Heat of water adsorption						achieved
9							Adsorption Regeneration tests						achieved
10										Assessment of process cost and scale-up			achieved
11											Final Report		achieved

- Milestone **1**. Research teams were put in place.
- Milestone **2**. Laboratory synthesis of triamine-grafted pore-expanded mesoporous silica was achieved at the scale of ca. 10 g.
- Milestone **3**. A 200 g batch was successfully prepared at the University of Ottawa (p. 1-2). A 130 g sample was sent to PNNL on June 29, 2012; then 40 g at a later date.
- Milestone **4**. Characterization of triamine-grafted pore-expanded silica was achieved using N_2 adsorption, TGA, solid state NMR, SEM, FTIR and CO_2 adsorption. The material met all the expectations (loading: 8.06 mmol N/g; CO_2 capacity: 9.48 % at 25 °C, and 8.03 % at 50 °C). The material was stable in the presence of water vapour and oxygen under relevant conditions (p. 2-7).
  The material did not tolerate SO_2. Parallel effort led to the development of novel SO_2 selective adsorbents (p. 7-10).
  A second material (40 g) consisting of polyethylenimine(PEI)-impregnated nanoporous silica was supplied to PNNL. (p. 10-11).
- Milestone **5**. Achieved. Detailed description in page (11-12).
- Milestone **7**. Debugging and testing (gas and liquid leakage, heating, cooling, etc) is described in page (12).
- Milestone **8**. Achieved. The heat of water adsorption was found to be ca 2700 kJ/kg.
- Milestone **9**. Detailed test program in the microstructured bed at PNNL exploring the effect of flow rate, gas composition, heating and cooling rate, and reactor pressure is provided in pages (16-32).
- Milestone **10**. Process design and CFD modeling of the structured bed was carried out to simulate the temperature profiles throughout the bed (p. 35-51).

SUMMARY AND RECOMMENDATIONS FOR FUTURE WORK

The amine-grafted adsorbent in a packed particle bed of 250 μm average particle size showed around 10 wt.% working capacity in 4-min adsorption/nitrogen cycles over a temperature range of 22 to 55 ^{o}C. This is an excellent adsorbent compared to the published literature data.

The protocols for fabrication and testing of the structured bed module have been developed. The abilities to conduct rapid thermal swing, pressure swing, and combined thermal and pressure swing with the structured bed module have been demonstrated, which is a unique research capability to generate adsorption/regeneration kinetics data by directly using powder materials.

The best CO_2 working capacity demonstrated with the structured bed is about 7.5 wt%, and CO_2 working capacity of 3 to 5 wt% in the structured bed has been repeatedly obtained with a large number adsorption/regeneration cycles (up to 220). The concept of rapid adsorption/regeneration swing is shown.

It appears that the amine-grafted adsorbent material was sensitive to the experimental procedures. It could be completely deactivated when the adsorbent was left in the residual testing environment for a long time. The lower CO_2 working capacity obtained in the structured bed likely results from the thicker adsorbent plate used in this work than the particle size and less temperature uniformity in the structured bed than the particle bed. The adsorbent plate thickness is 1.0mm versus 0.25mm particle size. Thus, diffusion resistance into the adsorbent plate is four times of the particle. The height of the structured bed is 20mm versus 10mm internal diameter of the particle bed, which means the thermal conduction distance in the structured bed is two times of the particle bed. The adsorbent loading in the structured bed was about 14-18g versus 6.64 g in the particle bed. As a result, the heat transfer effect is more pronounced in the structured bed than in the particle bed.

Based on our previous texting experiences, 13X zeolite powder in the structured bed can have same or even better CO_2 adsorption working capacity than the particle bed if the adsorbent plate thickness is small enough (~300 μm). It is expected that the CO_2 working capacity of the amine-grafted adsorbent in the structured bed of thinner plates should match the particle bed.

Testing of PEI-impregnated silica adsorbent in the structured bed shows 1 – 1.5 wt% CO_2 working capacity. Thus, this adsorbent material is not recommended.

The theoretical analysis indicates it is not possible to have an adsorbent that can be regenerated by heating up in 1 bar of CO_2 with high CO_2 working capacity and low heat of adsorption at the same time. The adsorbent must have the heat of adsorption large enough to be regenerated by heating up in 1 bar CO_2. Then, fundamentally, the energy consumption for an adsorption process would be same to the amine scrubbing process. It is not clear how the energy saving could be realized using the thermal swing adsorption process. No literature data showing the adsorbent regeneration in 1 bar of CO_2 has been found.

Regeneration of the amine-grafted adsorbent in this work always replies on reduction of partial pressure of CO_2 (in N_2 purge or vacuum). Thus, a vacuum pressure swing adsorption process is proposed for process economics analysis of CO_2 capture in a 550 MWe coal-fired power plant. No steam is needed in the proposed process, which is the largest saving compared to the amine process. For burning of the same amount of coal, 13.5% more power output can be produced with the adsorption process than the amine capture. Further enhancement of energy efficiency will be subject to thermodynamic limitation, since a large amount of power is always needed to produce high-pressure CO_2 for sequestration purposes out of low-pressure 15% CO_2 flue gas mixtures. The capital cost with the adsorption process is estimated to be $312 and $256/kW for 3.5 wt% and 7.0 wt% CO_2 working capacity, respectively, which is much less than $790-950/kW estimated for the amine process. Doubling CO_2 working capacity would proportionally reduce the adsorbent size and lower the associated capital cost. However, capital costs associated with the CO_2 compression system would not be affected by the CO_2 working capacity. The variable operation cost is dominated by the electricity consumption to drive the separation process. The adsorbent cost is minor as long as the adsorbent has a reasonable lifetime such as >5 years.

Future work

This seeding project enables confirmation of the adsorbent material performances and demonstration of structured bed concepts for rapid adsorption/regeneration cycles (~3min). Meanwhile, new problems are revealed. The following research subjects are recommended for further development.

- Understand operation windows of the amine-grafted adsorbent material. For example, characterization of the adsorbent structure and activity after it is treated under various temperatures and gas environments.
- Make and deliver robust adsorbent materials.
- Develop adsorption and regeneration kinetics of the adsorbent material. For example, the adsorption can be measured on TGA/DSC apparatus with online Mass spec analyzer to quantify impacts of the feed gas composition and temperature on the adsorption loading and heat of adsorption, particularly pertinent to moisture effects. This kind of studies were performed at PNNL for other projects, which is an efficient way to obtain kinetics useful to an actual adsorption/desorption process
- Optimize the thickness and channel spacing of the structured bed to achieve the same performance as the adsorbent particle.
- Increase the structured bed length and volume to have neat separation and produce a pure CO_2 stream from regeneration.
- Validate the key assumptions made in the present process economics analysis.

TABLE OF CONTENTS

DETAILED REPORT

OBJECTIVES

This is a collaboartive project bewteen the University of Ottawa (UO) and Pacific Northwest National Laboratory (PNNL). The ultimate objective of this project is to demonstrate the competitive advantages of PNNL's unique micro-structured adsorption beds loaded with state-of-the-art UO's adsorbents for CO_2 capture from flue gas. The short-term objective to be achieved in the current stage is to carry out material synthesis and characterization as well as laboratory testing of adsorption/regeneration processes to obtain critical performance data required for process design and economic evaluation.

This report describes progress achieved by the UO and PNNL research group since the start of this project on June 1, 2012.

BACKGROUND INFORMATION

It is proposed that two materials, namely a triamine-grafted pore-expanded MCM-41, and a polyethylenimine-impregnated nanoporous material be developed at the University of the Ottawa. This includes the design, synthesis, characterization and laboratory evaluation of the materials. It also includes the preparation of ca. 100 g of each material to be supplied to PNNL. The PNNL group will carry out adsorption-desorption studies in microstructured beds as well as preliminary process design.

As described below, the first material was synthesized in a sufficient amount, and a batch of 130 g was sent to PNNL on June 29, 2012 along with key characterization data. The development of the second material is well underway.

DETAILED PROGRESS REPORT

I. Development of Triamine-grafted Pore-expanded MCM 41 Adsorbent (TRI-PE-MCM-41)

1.1. Synthesis of triamine-grafted pore-expanded MCM-41

The pore-expanded MCM 41 (PE-MCM-41) silica was prepared using a two-step procedure involving the preparation of a conventional MCM-41 silica at low temperature in the presence of structure-directing agent cetyltrimethylammonium bromide, followed by pore-expansion in the presence of decyldimethylamine (DMDA). An amount of 578.6 of tetramethylammonium hydroxide (25 % in water) was mixed with 5.5 L of water under vigorous stirring in a 8 L stainless steel vessel. An amount of 820 g of CTAB was subsequently added, and stirred for 15 min. Then, 328.4 g of Cab-O-Sil fumed silica was added. After stirring for 30 more minutes, the resulting gel was heated under autogeneous pressure at 100 °C for 40 h. The obtained material was separated by vacuum filtration, washed thoroughly with water and dried at ambient conditions.

As for pore-expansion, 350 g of as-synthesized MCM-41 was added under vigorous stirring to a suspension of 437.5 g of DMDA in 5.25 L of water. The resulting mixture was heated under

autogeneous pressure at 130 °C for 72 h. The material was then separated by filtration, washed and dried in ambient condition. To remove the template and the pore-expander, the material was calcined under flowing nitrogen while the temperature increased to 550 °C (1 °C/min), then in oxygen at 550 °C for 5 h. The obtained material is designated as PE-MCM-41.

The grafting of triamine on pore-expanded MCM 41 was carried out in a batch reactor using 100 g of pore-expanded MCM 41. The support was pre-dried in a vacuum oven at 120 °C for 2 h. The material was then poured in a 8 L stainless steel vessel containing 1.5 L of toluene. The mixture was homogenized by stirring, then 4 mL of water was added every 30 min to a total volume of 20 mL. Subsequently, 300 mL of triaminesilane was added under vigorous stirring. The reactor vessel was then closed and stirred for 16 h in an oven at 85 °C. The resulting material was separated by filtration and washed with toluene and pentane. The obtained solid material was dried at 100 °C in a convection oven for 1 h. This final solid material was termed as TRI-PE-MCM-41.

1.2. Characterization of TRI-PE-MCM-41

The structural characterization of PE-MCM-41 and TRI-PE-MCM-41 was carried out by nitrogen adsorption-desorption at 77 K using a Micromeritics ASAP 2020 adsorption analyzer. Before adsorption measurements, PE-MCM-41 was degassed under vacuum (1×10^{-5} Torr) at 150 °C for 3 h, whereas, the organically-modified material was outgassed at 100°C to prevent any potential thermal decomposition. The BET surface areas were calculated from the N_2 adsorption isotherms in the relative pressure (P/P_0) range from 0.05 to 0.20. The pore size distributions (PSD) were calculated from the adsorption branch using the Barrett–Joyner–Halenda (BJH) method with Kruk–Jaroniec–Sayari (KJS) correction, and the maximum of the PSD was considered as the average pore size. The pore volume was considered as the volume of liquid N_2 adsorbed at P/P_0 = *ca*. 1.

Scanning electron microscopy (SEM) images were recorded on a JSM-7500F FESEM (JEOL) instrument operated at 1 keV, to determine the particle size and the morphology of the materials. Samples in ethanol suspension were deposited on colloidal graphite and dried at room temperature.

FTIR spectra of materials were recorded on a Nicolet 6700 FTIR instrument equipped with a ATR module using KBr as background. The ^{13}C CP/MAS NMR spectrum was collected on a Bruker Avance 200 instrument. The spinning frequency was set to 4.5 kHz. The contact time was 2 ms, with recycle delays of 2 s.

The organic content of the materials was determined by thermogravimetric analysis (TGA) using a TA Q500 instrument. The sample was heated at 10 °C min^{-1} under N_2 up to 800 °C followed by decomposition in the presence of air at the same heating rate, up to 1000 °C. The weight loss below 200 °C was attributed to adsorbed water, solvent and any alcohol associated with non-hydrolyzed alkoxy groups. The organic content was calculated based on the weight loss beyond 200 °C at atmospheric pressure.

1.3. Adsorption measurements

CO_2 adsorption on TRI-PE-MCM-41 was carried out with 5 % CO_2 at different temperatures e.g. 25 °C, 40 °C, 50 °C after pre-treatment under N_2 at 120 °C for 120 min using TGA Q500 instrument.

In separate experiments, it was shown elsewhere that at 5% CO_2, the chemisorption is fully achieved, whereas physisorption is still negligible.

The behaviour of the material over 100 cycles of adsorption (50 °C) in the presence of 15% CO_2/N_2 and desorption (120 °C) in N_2 purge gas, was examined under dry condition. A similar experiment was also conducted under humid condition (dew point = 20 °C) to check the effect of water.

1.4. Characterization results

1.4.1. Structural properties: N_2 adsorption-desorption measurements

The N_2 adsorption-desorption isotherms for PE-MCM-41 and TRI-PE-MCM-41 are presented in Figure 1 and 2, respectively with the corresponding BJH pore size distributions. The isotherms are characteristic of mesoporous materials with narrow pore size distributions. The data obtained for pore volume and pore size are listed in Table 1. The surface area, pore volume and pore size decreased after grafting, indicating that the organic modification took place on the internal surface of the material channels. Notice that after surface modification, TRI-PE-MCM-41 remained porous. This is a key requirement for high performance adsorbents.

Table 1. Structural properties of the materials

Material	S_{BET} (m^2/g)	Pore volume (cm^3/g)	Pore size (nm)
PE-MCM-41	992	2.19	9.9
TRI-PE-MCM-41	243	0.50	8.2

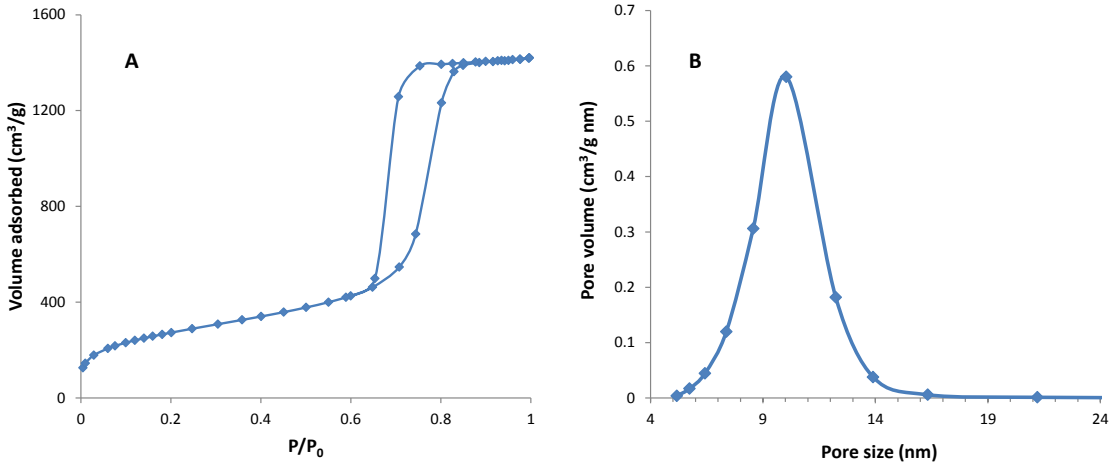

Figure 1. (a) Nitrogen adsorption-desorption isotherm for PE-MCM-41, and (b) the corresponding pore-size distribution

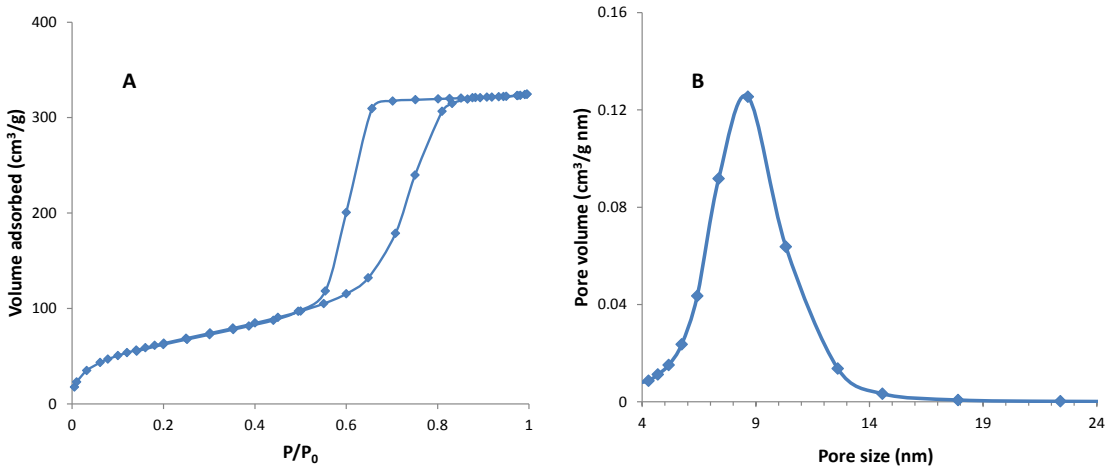

Figure 2. (a) Nitrogen adsorption-desorption isotherm for TRI-PE-MCM-41, and (b) the corresponding pore-size distribution

1.4.2. Particle morphology: Scanning electron microscopy (SEM)

A typical SEM image of PE-MCM-41 is shown in Figure 3. As seen the material is comprised of particles of similar shapes and sizes. The average particle size was *ca.* 25 μm.

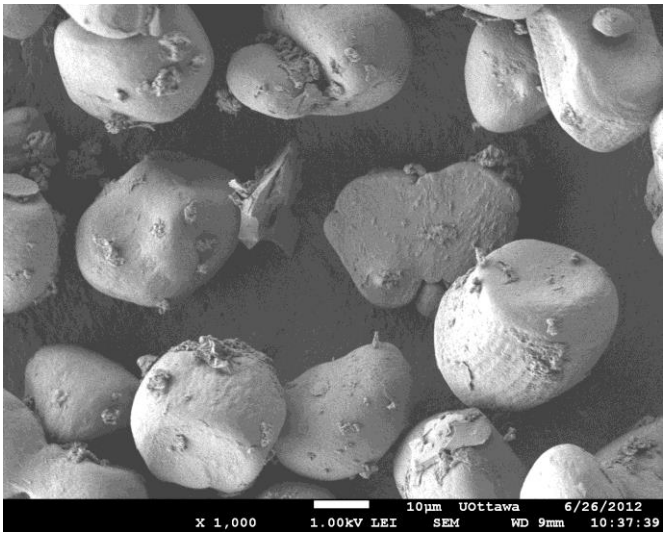

Figure 3. SEM image for TRI-PE-MCM-41

1.4.3. FTIR results

As shown in Table 2 and Figure 4, FTIR data are consistent with the occurrence of amine groups in TRI-PE-MCM-41.

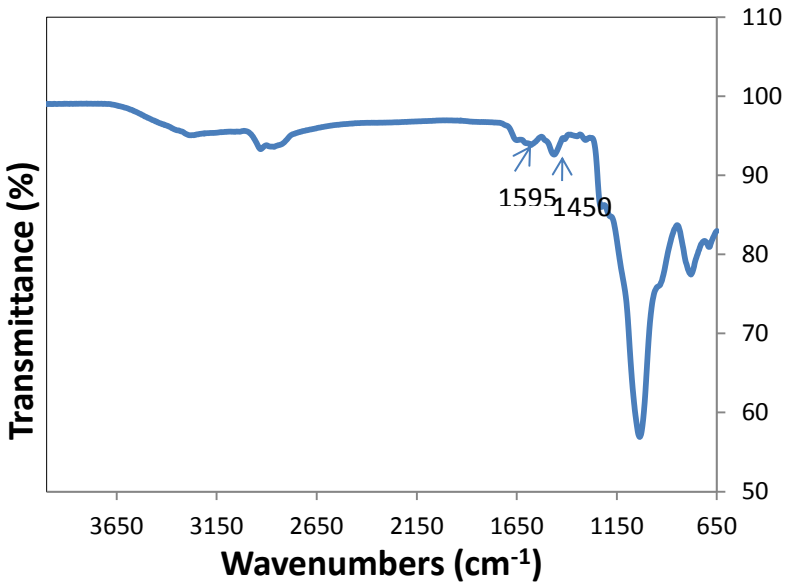

Figure 4. FTIR spectrum for TRI-PE-MCM-41

Table 2. FTIR data for TRI-PE-MCM-41

Wavenumbers	Assignment
1450 cm^{-1}	CH_2 deformation
1595 cm^{-1}	NH_2 deformation
2815-2940 cm^{-1}	CH_2 stretching

1.4.4. ^{13}C CP/MAS NMR data

The ^{13}C CP/MAS NMR spectrum of TRI-PE-MCM-41 is shown in Figure 5. TRI-PE-MCM-41 exhibits signals below 70 ppm corresponding to the different carbon atoms present in the triamine (see inset). In addition, a small signal at ca. 164.6 ppm corresponds to carbamate associated with CO_2 adsorption from ambient air.

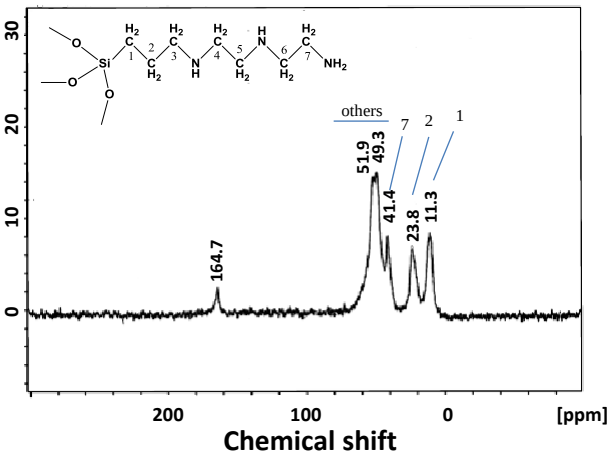

Figure 5. ^{13}C CP NMR spectrum for TRI-PE-MCM-41

1.5. CO_2 adsorption measurements

The organic content determined using TGA is 38.69 % from which nitrogen 'N' content of the material calculated is 8.06 mmol N/ g. The adsorption capacities observed with 5 % CO_2/N_2 at different temperature are mentioned in Table 3.

Table 3. Adsorption capacity of TRI-PE-MCM-41 at different temperature using 5 % CO_2/N_2

Adsorption temperature (°C)	CO_2 adsorption (wt%)
25	9.48
40	8.78
50	8.03

1.6. Stability of the TRI-PE-MCM-41

1.6.1. Cycling behaviour of TRI-PE-MCM-41

The working capacity examined by 100 adsorption (50 °C) / desorption (120 °C) cycles under dry condition with 15 % CO_2/N_2. As seen in the Figure 6 adsorbent is deactivated gradually and percent loss of adsorption capacity after 100 cycles is 16%.

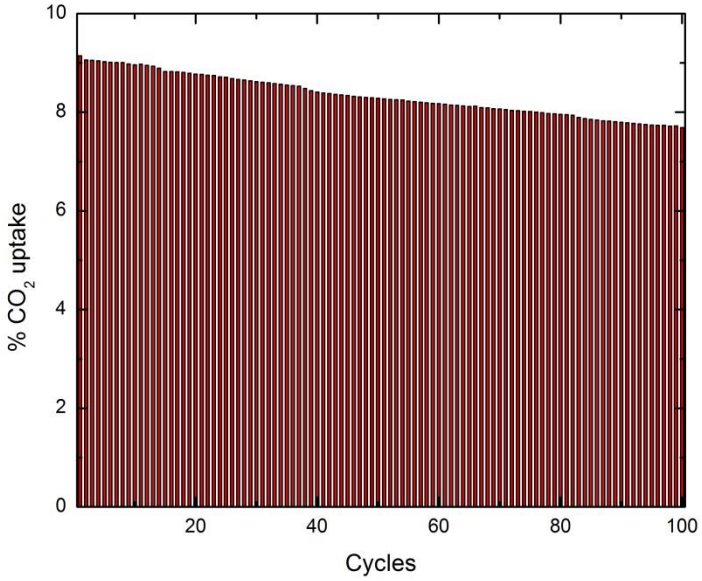

Figure 6. Adsorption-desorption cycles using 15 % CO_2/N_2 over TRI-PE-MCM-41 in dry condition using a temperature swing procedure with adsorption at 50 °C and desorption at 120 °C under flowing N_2

It was demonstrated elsewhere that deactivation of amine-containing materials in the presence of dry CO_2 was due to the gradual formation of urea linkages, which are stable under common desorption conditions. To overcome this deactivation, it was essential to humidify the feed and purge gas. For comparison, a similar cycling experiment involving 100 cycles of adsorption (15% CO_2/N_2; 50 °C,

18.91 % relative humidity) and desorption (N_2; 120 °C, 1.21 % RH) was carried out using. No deactivation was observed.

1.6.2. Effect of SO_2 and NO_2

The effect of SO_2 and NO_2 on CO_2 adsorption was investigated by the treatment of the adsorbent with dilute SO_2/N_2 or NO_2/N_2 mixtures for several hours at 50 °C in a dedicated system comprised of a 1/8" OD column located in a temperature-controlled oven, a series of mass flow controllers for feed flow and compositions adjustments, and a mass spectrometer (Cirrus from MKS) for gas analysis. The CO_2 adsorption was measured before and after the treatment using the TGA Q500 instrument. The data obtained are reported in Table 4 which indicate that the adsorbent deactivates irreversibly not only in the presence of SO_2/N_2 and NO_2/N_2 mixtures, but also in the presence of 50 ppm SO_2/N_2 in 14.2% CO_2/N_2. Therefore, it is critical to remove these impurities in order to maintain the potential of the adsorbent.

Table 4. Effect of SO_2 and NO_2 on TRI-PE-MCM-41

Gas composition	Exposure time	Temperature	CO_2 uptake loss
1000 ppm NO_2 + balance N_2	24 h	50 °C	96 %
100 ppm SO_2 + balance N_2	15 h	50 °C	65 %
100 ppm SO_2 + 13.5% CO_2 + balance N_2	15 h	50 °C	40 %
50 ppm SO_2 + 14.2 % CO_2 + balance N_2	30 h	50 °C	34 %

1.7. Development of a selective adsorbent for SO_2

A novel material containing grafted *N*,*N*-dimethylpropylamine was found to adsorb SO_2 reversibly, without adsorbing any CO_2. The material, obtained via grafting of dimethylamino-propyltrimethoxysilane onto PE-MCM-41, will be referred to as TER-PE-MCM-41. The amine loading as determined by TGA was 28 wt% (3.26 mmol/g).

The adsorption isotherms for TER-PE-MCM-41 (Figure 7) show that SO_2 uptake increases strongly versus the partial pressure increases up to 1000 ppm, indicating a relatively strong adsorbate-adsorbent interaction. Moreover, as expected the SO_2 uptake decreases as the temperature increases (Figure 8). Moreover, as shown in Figure 9, the SO_2 adsorption was fully reversible.

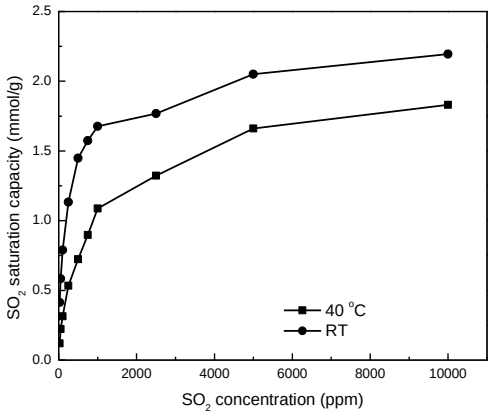

Figure 7. SO_2 adsorption isorthems over TER-PE-MCM-41 at 25 and 40 °C.

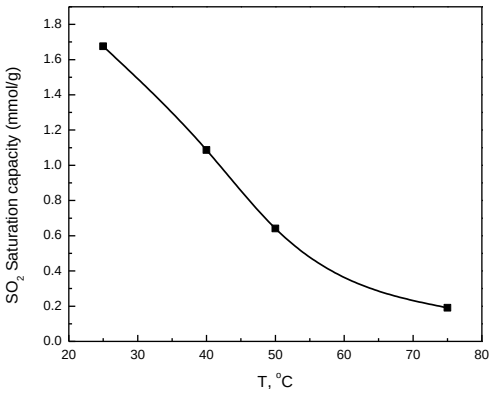

Figure 8. Effect of temperature on the saturation capacity of SO_2 over TER-PE-MCM 41 (Conditions: 0.1 % SO_2 + balance N_2, flow rate = 50 mL/min).

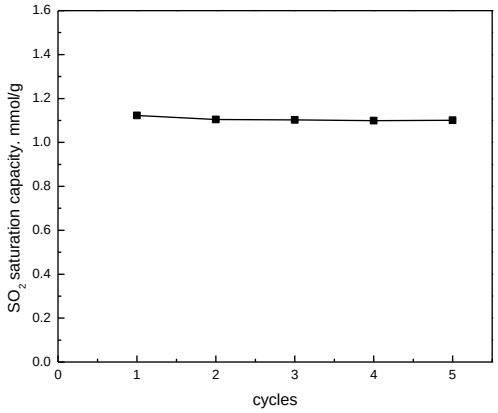

Figure 9. SO_2 Adsorption and regeneration cycles over TER-PE-MCM 41 (Conditions: adsorption: 0.025% SO_2 + balance N_2, flow rate = 50 mL/min; regeneration: under N_2 at 130 ^oC).

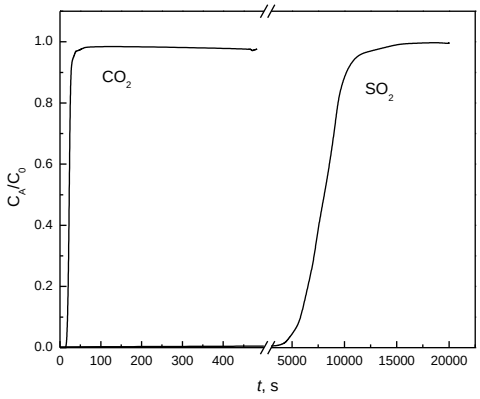

Figure 10. Selectivity of SO_2 in the presence of CO_2/N_2 (Condition: SO_2 concentration = 0.05% + 7.5% CO_2 + balance N_2, T = 40 ^oC, Flow rate = 50 mL/min).

Figure 10 shows the breakthrough curve for a gas mixture with the following composition: 0.05% SO_2 in 7.5% CO_2/N_2. As seen, CO_2 appeared in the column downstream almost immediately after the process has started, but no SO_2 was detected in the downstream for an

extended period of time, indicating that the adsorbent possesses a high efficiency for adsorption and separation of SO_2 in a CO_2-containing feed.

In the presence of water vapour, the SO_2 adsorption capacity increased significantly. Figure 11 shows that in the presence of 0.025% SO_2 in N_2, the adsorption capacity was 0.52 mmol/g at 40 ^oC; whereas in the presence of water vapour (dew point = 20 ^oC), under otherwise the same conditions, the SO_2 uptake increased threefold to 1.5 mmol/g.

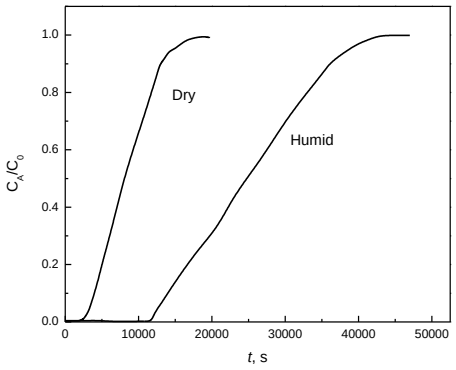

Figure 11. Effect of water vapour on SO_2 adsorption over TER-PE-MCM 41 (Conditions: 0.025 % SO_2 + balance N_2, 31.8 % RH, flow rate = 50 mL/min).

In a second stage, we focused on the development of materials with higher density of tertiary amine groups, but without any primary or secondary amines. Since such materials are not commercially available, we had to modify some existing amine-containing dendrimers (Figure 12) and polymers (Figure 13).

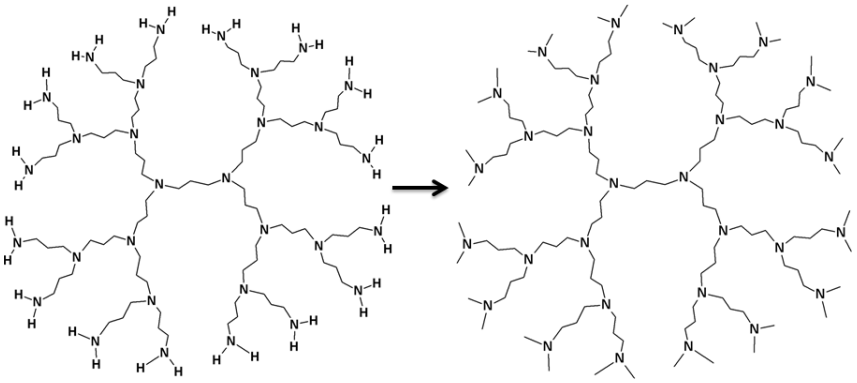

Figure 12. Polypropylamine dendrimer

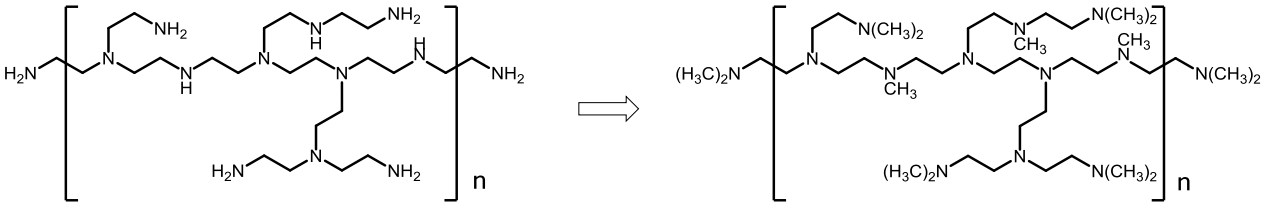

Figure 13. Branched polyethylenimine

We first started with Generation 2 and Generation 3 polypropylamine dendrimers (PPI, Figure 12), which have an outer shell of primary amine groups, and we developed a synthetic method to change such amines into tertiary amines, as shown on the right-hand side of Figure 12. As far as SO_2 adsorption is concerned, such materials behaved like grafted tertiary amine (TER-PE-MCM-41), except that the SO_2 uptake was much greater (*vide infra*).

In a further step, we used much cheaper branched polyethylenimine (PEI) as a starting material. PEI is a mixed polyamine containing primary, secondary and tertiary amines in a 33:40:27 molar ratio. We developed a chemical procedure to change most, if not all primary and secondary amines into tertiary amines (Figure 13).

Modified PPI and modified PEI were loaded on different nanoporous silicas, including SBA-15 and ethanol-extracted pore-expanded MCM-41. Typical comparisons of SO_2 uptake over the three materials are shown in Figure 14. A single SO_2 concentration is shown for illustration. It is seen that in the presence of 0.1% SO_2:N_2 at 25 °C, the uptake increased from 1.7 mmol/g for TER-PE-MCM-41 to 4.6 mmol/g for modified PEI on ethanol-extracted PE-MCM41. We believe that this is a major achievement.

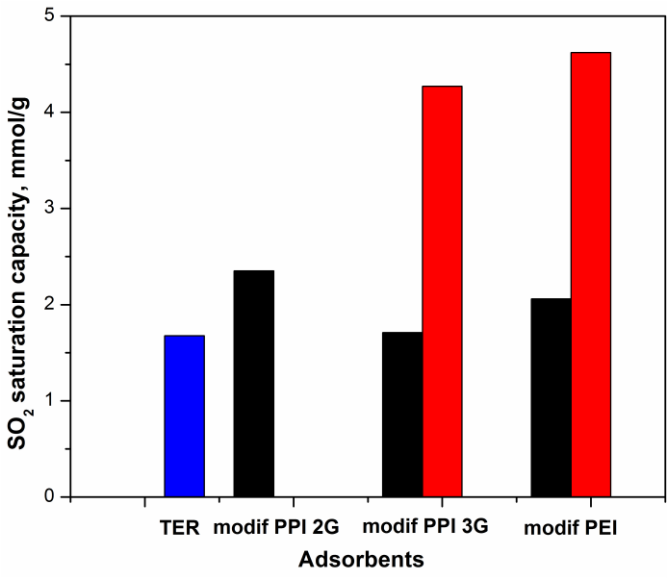

Figure 14. Dry SO_2 adsorption at room temperature for different adsorbents (0.1 % SO_2/N_2, total flow rate = 50 mL/min).

II. Polyethylenimine-supported Nanoporous Silica

While amine-grafting is an excellent methodology to design adsorbent with high rate of adsorption because the adsorption sites are readily accessible of the internal surface of the support, the amine loading is often limited by the surface density of OH groups on the surface. However, impregnation of amine-rich molecules such as polyethylenimine (PEI) allows much higher amine loadings in materials with high pore volumes, and with greater control. Moreover, the impregnation procedure is easier and less costly than surface grafting. The drawback of heavily loaded PEI-based materials is the occurrence of excessive diffusion resistance, thus limiting the rate of adsorption, and ultimately the CO_2 uptake. To mitigate the diffusion resistance, attempts were made to use nanoporous supports with larger surface areas, larger pore volumes, and/or larger pore sizes. Although all these factors were shown to have a positive impact on the adsorptive properties, none was fully satisfactory. Our approach was to use nanoporous silica ideally with large surface area, pore volume and size, but most importantly with small particle size and short diffusion path, i.e., pore length.

Figure 15 provide typical images for nanoporous silica with platelet morphology suitable for PEI impregnation.

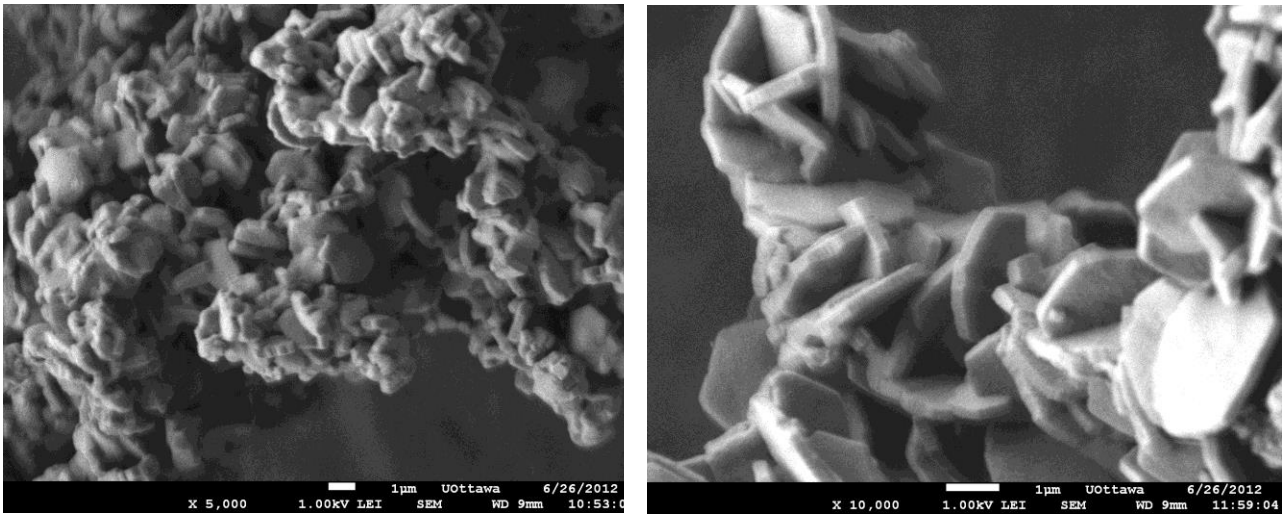

Figure 15. typical SEM images for nanoporous silica with platelet morphology.

III. Adsorption and regeneration studies in micro-structured adsorbent beds

(Task 3, PNNL)

3.1 Testing apparatus

All the adsorption tests in this work were performed on the adsorption testing cart (Figure 16) in PNNL's Carbon Capture Laboratory, which was built from previous PNNL internal investment. The testing cart was originally designed and used for testing of conventional adsorbent particles in a volume of a few liters, which was operated with a typical adsorption and regeneration cycle time of a few hours. To conduct rapid adsorption/desorption tests, the testing system was modified under PNNL's internal support. The modifications included removal of one of the two currently installed packed sorbent beds and addition of necessary connection fittings for incorporation of the structured bed module into the system. The existing heat-trace elements and thermal insulation was removed and reinstalled. The fluid connections of the existing sorbent bed jacket were modified to allow switching between a hot and cold bath using a pair of existing pneumatically-actuated 3-way valves.

Figure 16. CO_2 adsorption testing cart

The testing system is equipped with on-line Mass spec and infrared spectroscopic analyzers. The system is controlled by a computer for un-attended operation. The general testing procedure is outlined as follows:

(1) Conduct gas leakage tests of the testing module under a positive pressure (10psig)
(2) Conduct gas leakage tests of the testing module under vacuum (~10 torr)
(3) Conduct liquid leakage tests of the testing module with circulation of heat exchange fluid at the highest flow rate and at different temperatures
(4) Conduct heating/cooling tests of the testing module with the heat exchange fluid with inert N_2 gas passing through the adsorbent bed at a flow rate about 4 liter/min to determine how quickly the module can be heated up and cooled down from 50 to 120 ^oC
(5) If all the above tests passed, start the adsorption test
(6) Set the heating and cooling fluid at respective targeted temperatures
(7) Introduce the CO_2 gas mixture
(8) Monitor the bed temperatures, gas inlet and outlet temperatures, heat exchanging fluid temperature, reactor pressure, and exit gas compositions.
(9) Stop the adsorption run at a certain time.
(10) Start regeneration

Since the highest regeneration temperature used in the previous studies of the amine-grafted adsorbent was at 120 ^oC in N_2 gas purge, the regeneration temperature tested in this work was controlled not exceeding this temperature.

3.2 Testing of pelletized adsorbent particles in tubular heat exchanger reactor

To establish the baseline performances and also check potential impact of isopropanol on the adsorbent, we prepared and tested the adsorbent material in a particle form. An adequate amount of isopropanol was added into the as-received adsorbent powder to form a wet cake. The wet cake was pressed into pellets that were crushed and sieved into 45 -100 mesh. The sieved particle was packed into a stainless steel reactor tube of ½" OD. The reactor tube was sheathed in a 1" OD tube for introduction of heat exchanging fluid. Two thermocouples were placed at the top and bottom of the bed to monitor the bed temperature. The packed bed information is listed in Table 1.

Table 1. Packed adsorbent particle bed

Sorbent weight, g	6.64
Packed volume, cc	13.7
Particle size min, μm	150
Particle size max, μm	355
Bed tube OD, in	0.5
Bed tube thickness, in	0.048
Bed diameter, cm	1.03
Bed height, cm	13.4

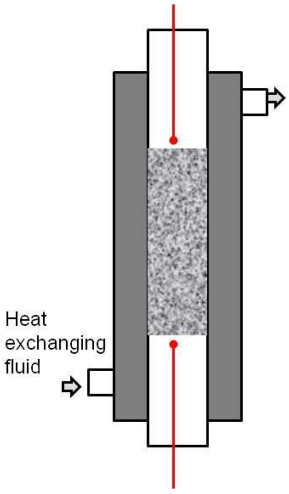

Isothermal adsorption/desorption tests were performed with this particle bed. The bed temperature was controlled by pumping the heat exchanging fluid of constant temperature. The following adsorption and desorption gas compositions were used.

- Simulated feed gas for adsorption: dry gas stream of 15% CO_2, 5% He, and balance N_2; humidified to 50% RH at adsorption temperature
- Regeneration gas purge: a dry gas stream of 5% He and balance N_2; humidified to 50% RH at room temperature

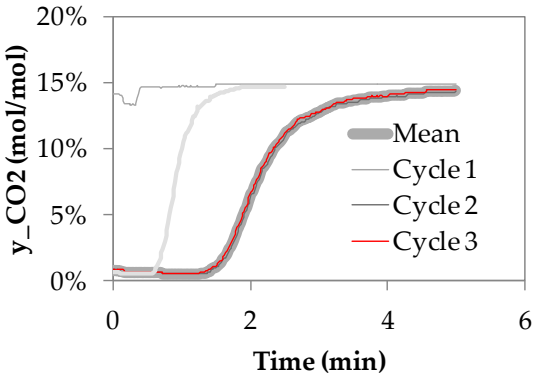

(a). Adsorption breakthrough profile

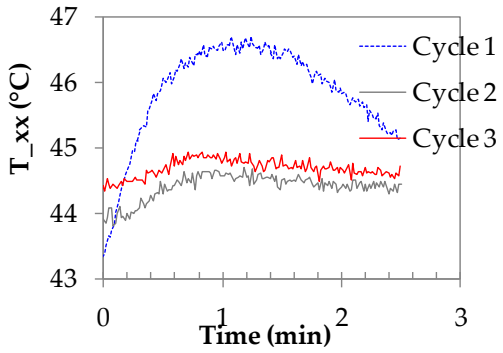

(b). Top bed temperature

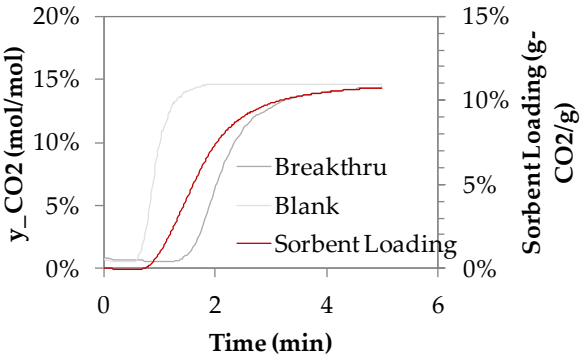

(c). CO_2 loading calculation

Figure 17. Isothermal adsorption testing results of the adsorbent particle bed (heating jacket temp 45°C)

The representative testing results are shown in Figure 17. The heating jacket temperature was maintained at 45°C during adsorption and regeneration. The regeneration was conducted using N_2 gas. Both adsorption and desorption were performed under nearly atmospheric pressure. The adsorption and regeneration was switched every 5 minute. The substantial breakthrough occurred at about 3min. The adsorption breakthrough profiles overlap for three consequent runs, which indicate effective regeneration of the adsorbent by N_2 purge. A few degrees of temperature rise-up at the top of the bed occurred in first adsorption cycle, and the bed temperature got stabilized in the latter two cycles. Thus, the temperature rise-up was likely caused by irreversible adsorption in first run, such as adsorption of moisture. The CO_2 loading is calculated by integrating the breakthrough curve. The adsorbent bed was tested at three different temperatures as listed in Table 2.

The CO_2 loading measured from this work is around 10 wt%, which is very good compared to the other adsorbent materials reported in the literature and is consistent with the values provided University of Ottawa. The CO_2 loading slightly decreases with increasing temperature, which suggests that the adsorption is not so sensitive to temperature. After the adsorbent bed was stored in the testing system for a few weeks during the holiday time, however, re-testing of the same adsorbent bed resulted in a very low CO_2 loading (1.4 wt. %). Then, the adsorbent was unloaded from the reactor tube. It was found that the adsorbent material (Figure 18) looked yellowish compared to the fresh white powder and adsorbent particles formed large agglomerates as compared to fresh loose powder. We think that the adsorbent particles may have been exposed to water condensed from the residual gas in the testing system and the condensed water caused reaction of the amine functional materials.

Table 2. CO_2 working capacity of adsorbent particles measured in this work

Adsorption temp (^oC)	PNNL tests			Data provided by UO
	CO_2 loading (wt %)	Date	Note	CO_2 loading (wt %) in 5% CO_2/N_2
25	12.0	14-Dec	First run	9.48
25	11.9	15-Dec	repeat	
40				8.78
45	10.5	7-Dec	the same bed	
50				8.03
55	9.7	8-Dec	the same bed	
45	1.4	15-Jan	Check of the same bed	

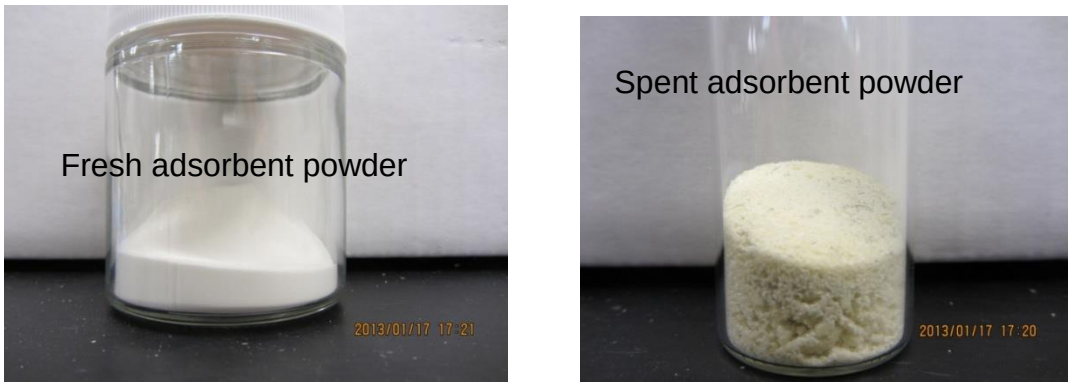

Figure 18. Appearance of adsorbent materials before and after testing

3.3 Package of the structured bed through layer-to-layer bonding for testing of amine-grafted adsorbent powder

First version of the testing module (Figure 19) comprises ten identical adsorbent plates being stacked with a metal spacer inside an aluminum vessel. An adsorbent plate was made by attaching a porous metal sheet onto one side of a support frame, which was made of Al metal as well, spreading a layer of adsorbent/iso-propanol paste uniformly on the metal sheet, and covering the adsorbent powder with another porous metal sheet. The porous metal sheet is made of NiCu alloy, is 27 μm-thick, and has average 48.8% porosity with sub-micrometer pore sizes. The pore size is small enough to get the adsorbent powder fully contained, and is large enough for gas to diffuse freely. The active area of the adsorbent plate, i.e., exposed to feed gas flow, is 4cm x 10cm = 40 cm^2. The adsorbent thickness is 1.0mm in average.

The individual adsorbent places were bonded together by placing corrugated Al meshes as spacers. The spacing between two adsorbent plates is 1.0mm. The adsorbent plates were sandwiched with a bottom and cover Al plate to form channels for a heat exchanging fluid to flow over the top and bottom surface of the adsorbent plate stack. Two manifolds were attached to the plate stack to provide inlet and outlet ports for the heat exchanging fluid. Thus, a structured bed with cross-flow heat exchange was formed. Thermocouples were inserted into the open channels between the adsorbent plates. Then, the other two manifolds were attached to the stack for feed gas inlet and outlet, respectively.

The packing density of the as-received powder (Tri-PE-MCM-41, 130 g) measured by tapping into a graduated cylinder was about 0.42 g/cc, which is low compared to zeolite materials. The net adsorbent loading for each adsorbent plate for the structured bed is listed in Table 3. In total, 26.43 g of adsorbent powder was loaded into the testing module of net adsorbent packing volume of 40cc and total bed volume of 76 cc. Thus, an average adsorbent packing density is 0.66g/cc. This packing density was substantially higher than the powder packing density of 0.42 g/cc.

Table 3. Adsorbent loading in each plate (Tri-PE-MCM-41 adsorbent powder, Al mesh filler of 5.45% solid fraction, Al support frame, NiCu porous membrane sheet)

Plate #	ID	Adsorbent loading, g
1	159-7/156-2	2.34
2	159-5B/156-1	2.54
3	159-5/159-2B	2.46
4	159-6/147-6	2.61
5	159-8B/156-4B	2.45
6	159-8/147-6B	2.58
7	159-7B/147-8	2.87
8	147-2B/147-8B	3.08
9	147-2/156-3B	3.05
10	159-6B/159-2	2.45
	total	26.43

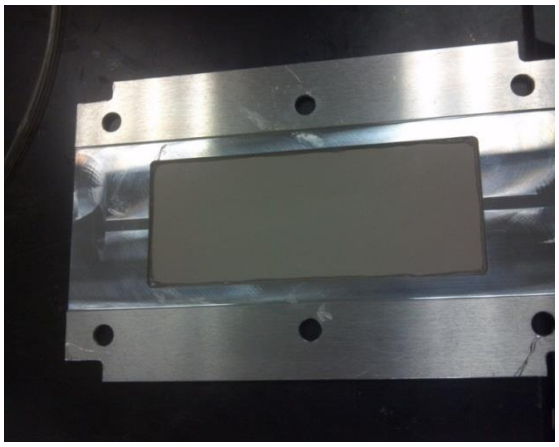

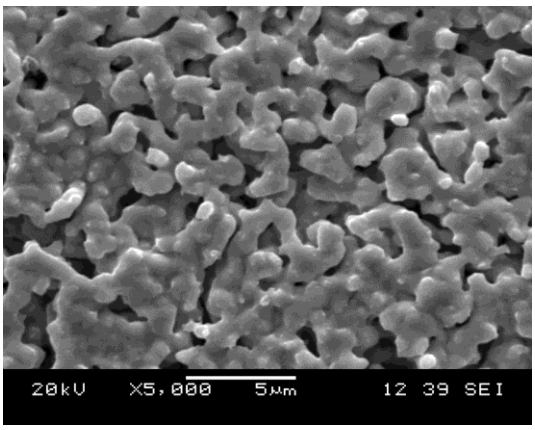

(a). An adsorbent plate with porous metal sheet cover (b). Surface of the porous metal sheet

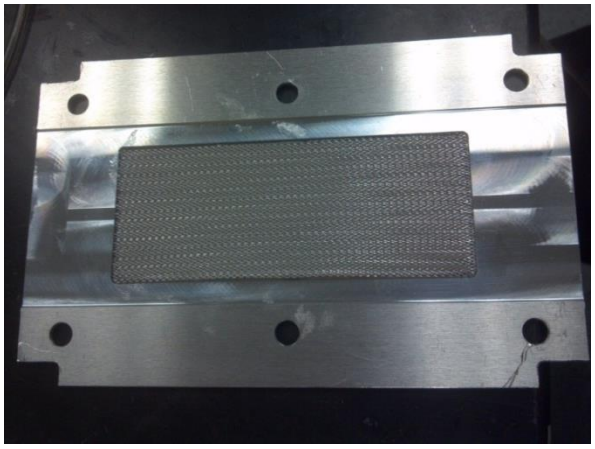

(b). Al mesh spacer of 95 % porosity

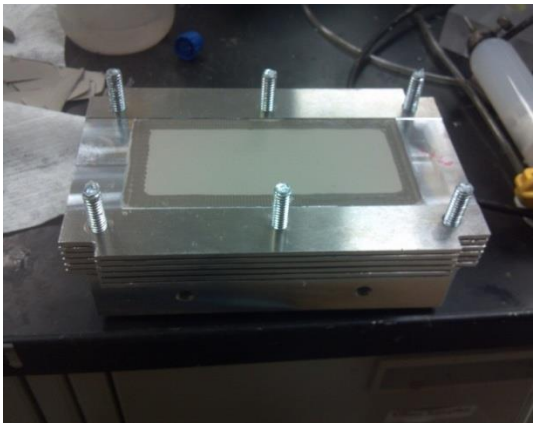

(c). Stacking of individual plates

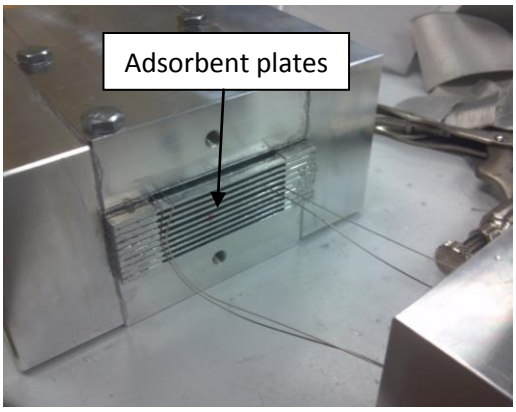

(d). Manifolds attached for heat exchange fluid

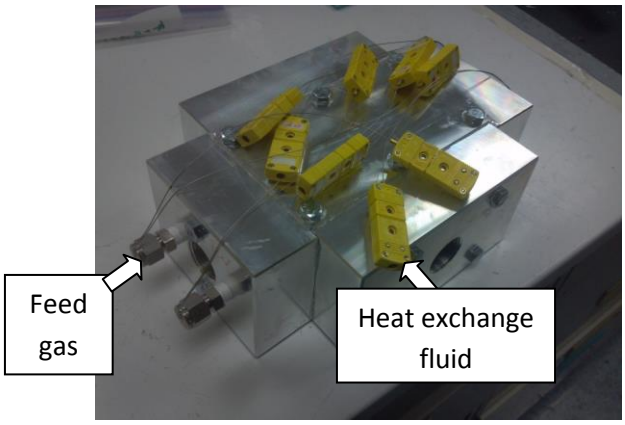

(e). Manifolds attached for feed gas in &out

Figure 19. First version of structured bed testing module (60036-163-CO2-10 plate) assembly

Placing an Al metal mesh into the adsorbent plate is to enhance the thermal conductivity. Silica materials have a fairly low thermal conductivity. The point-to-point contact in a conventional bead-packed bed substantially reduces the effective thermal conduction area. Due to high thermal conductivity of Al metal (200 w/m/K), incorporation of even 5 vol% Al metal into the adsorbent layer would increases the thermal conductivity from 1.1 W/M/K for the silica adsorbent to about 10 W/M/K for the adsorbent plate. It is estimated that a structured bed made in this way would provide enough thermal conductivity for effective heat transfer between the adsorbent bed and exterior heat exchanging fluid.

The spacers and interfaces between the adsorbent plate and heat exchanging fluid are made of aluminum metal to assure sufficient thermal conductivity. The expectation from this-

type package is to have intimate contact between the adsorbent plates and heat exchanging interfaces.

Gas leakage was detected in first trial and fixed. The following adsorption/regeneration runs were tried:

- Adiabatic bed at room temperature: adsorption and regeneration by N_2 gas purge
- Isothermal adsorption/N_2purge tests at different temperatures and feed gas flow rates
- Isothermal adsorption and vacuum regeneration

CO_2 loading only 2.2 wt% was obtained at room temperature at the beginning and dropped to about 1 wt% in later runs. It was found that ethylene glycol - heat exchanging fluid leaked from the jacket into the bed during vacuum swing operation. As a result, this reactor design was abandoned

3.4. Package of the structured bed using rectangle tubular reactor cartridge for testing of amine-grafted adsorbent powder

A new version of reactor (Figure 20) was fabricated using two Al rectangle tubes of different interior sizes. A heating jacket was formed by welding the two tubes together. The individual adsorbent plates were bundled together and inserted into the cavity. The plate height needs to be properly sized to minimize air gap between the top adsorbent plate and reactor wall. Only 7 adsorbent plates can be packaged into this reactor. The average adsorbent loading was 2.0 g/each plate, and the total adsorbent loading was 14.0 g.

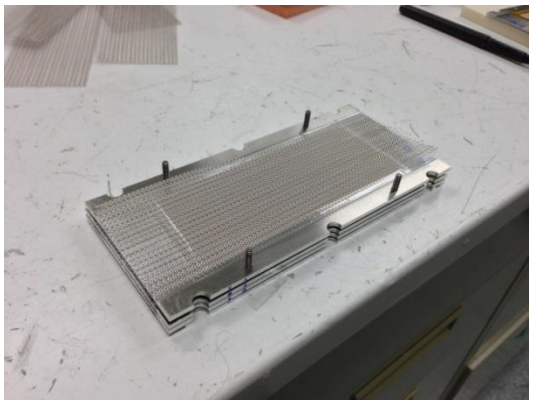

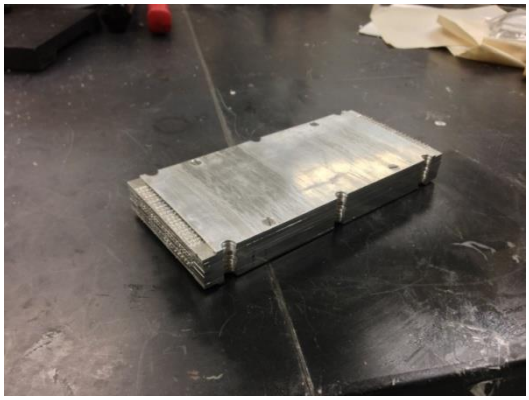

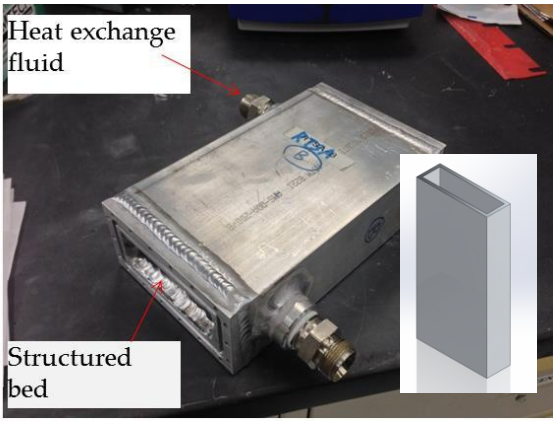

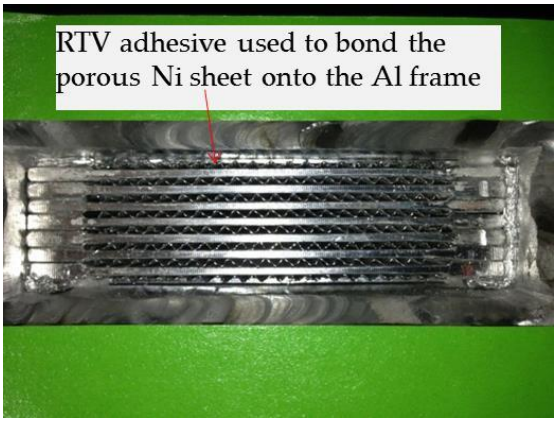

Figure 20. Second version of structured bed testing module (**61445-1-CO2-7 plate**)

Compared to the previous module, the new design makes the adsorbent be easily changed over. In addition, the Al weight or thermal mass of the reactor was dramatically reduced. Two four-point thermocouples were inserted into the middle of the structured bed to monitor the temperature distribution (Figure 21). The reactor module was insulated and mounted onto the test skid.

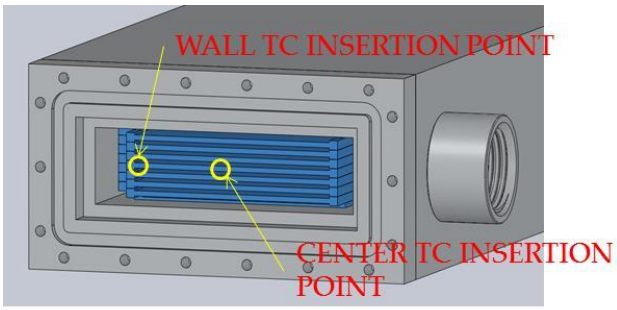

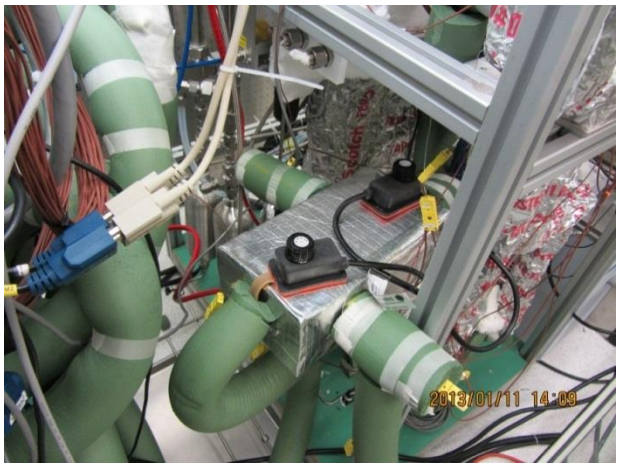

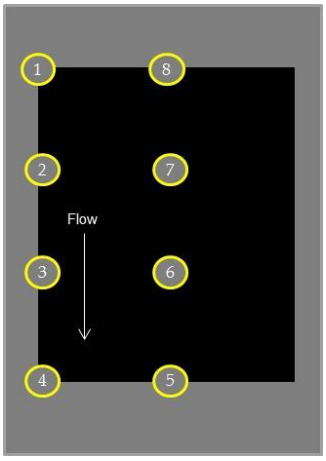

Figure 21. Installation of cartridge testing module on the testing system

One common problem for testing of packed adsorption beds at different temperatures is slow heating and cooling. To check how rapidly the structured bed can be heated up and cooled down, the structured bed was first tested in a flowing nitrogen gas without any CO_2 adsorption being involved. The heating and cooling was conducted by introducing a respective hot and cold heat-exchanging fluid. Variations of the mid bed temperature with time for different heating/cooling cycles are shown in Figure 22. The bed temperature can be switched between about 40 and 60 ^oC in 5 minute with respective 25 ^oC cold and 75 ^oC hot fluid. The bed temperature can be switched over a little broader range with 10-min cycle time. For a given reactor system and fluid temperature, the thermal transfer rate is proportional to the temperature differential between the fluid and the bed, which reduces with the time. Thus, a wider range of the bed temperature switch in a short time would require a larger temperature difference between the hot and heat fluid. It is noted that thermal mass in current testing module is still excessive due to relatively small volume of current adsorbent bed. The heating/cooling could be faster without excessive thermal mass.

Adsorption tests of this module were first conducted by keeping the heat jacket temperature at 25 ^oC. The regeneration was done with N_2 gas purge. The adsorption and regeneration profiles (Figure 23) for three 5-min adsorption and 5-min desorption sequential cycles overlap. The CO_2 loading calculated from the breakthrough curves is 6.8 wt%. The adsorption loading is increased to 7.6 wt% with 10-min desorption, which suggests that the adsorbed CO_2 was not fully desorbed in 5 min. It is worth noting that the mid bed temperature rises by 9 ^oC in the middle of adsorption due to heat of adsorption.

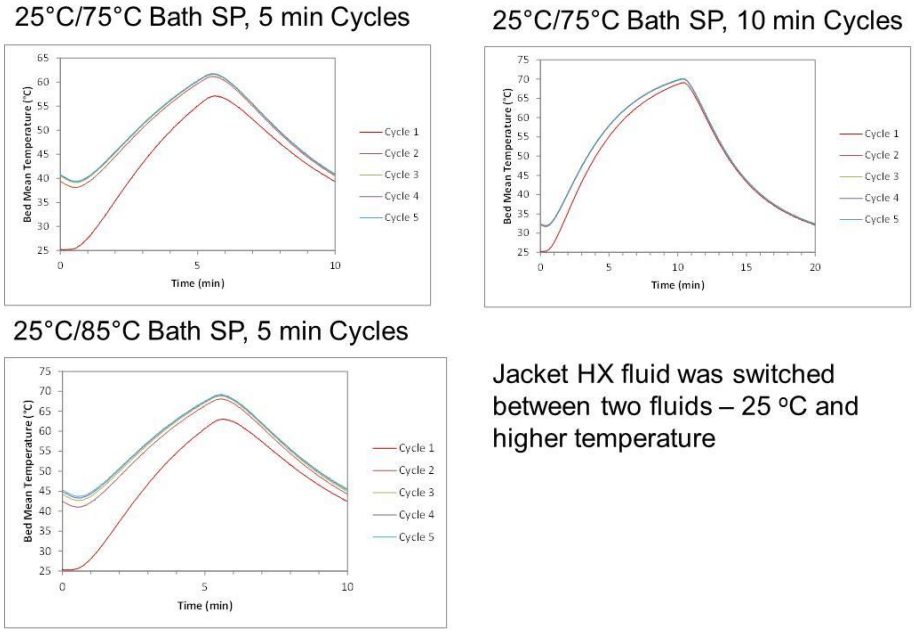

Figure 22. Heating and cooling of the structured bed by switching between hot and cold fluid in the jacket (no CO_2 adsorption, mid bed temperature)

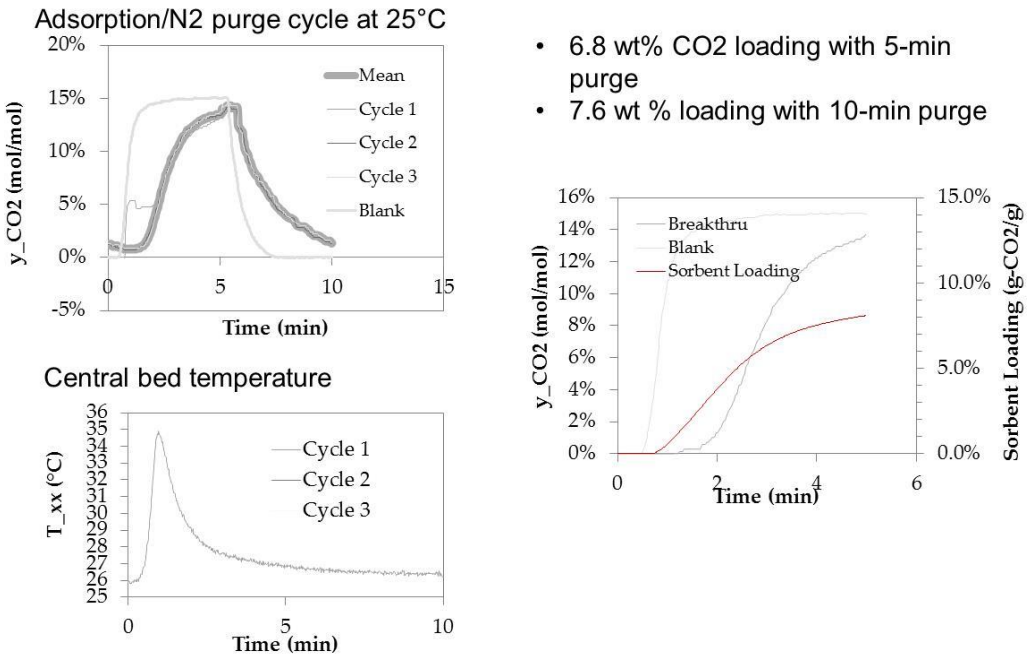

Figure 23. Adsorption testing results of structured bed module #61445-1-CO2-7 with 25^{o}C constant heat jacket temperature (tested on Dec. 21st)

Resulting CO_2 loading was less than the particle bed (12 wt%) at the same temperature, which could be explained by mass transfer limitation of the 1-mm thick adsorbent plate versus 0.25mm particle sizes. The structured bed performance was promising. This testing module was left idle during the holiday time. The testing was resumed with the same bed after the holiday. The isothermal measurements at 25 ^{o}C showed CO_2 loading of only 3 wt%. Then, the adsorption was run by increasing desorption temperature (Figure 24). The CO_2 loading was still low, within a range of 3 to 4 wt%. The initial adsorption activity could not be restored by increasing desorption temperature.

The testing bed was dismantled and the spent adsorbent was unloaded by peeling off the porous metal sheet (Figure 25). Compared to the whitish fresh adsorbent, the spent adsorbent looked yellowish and formed agglomerates. The spent adsorbent from the structured bed looked similar to the previous de-activated adsorbent particle. Thus, the adsorbent was deactivated during 2-week storage in the testing system. The possible cause could be similar to the particle bed, i.e., gradual degradation of the adsorbent material by condensation of residual moisture in the reactor system. The deactivated sorbent could not be recovered by heating and purging in N_2 gas, and by pulling vacuum.

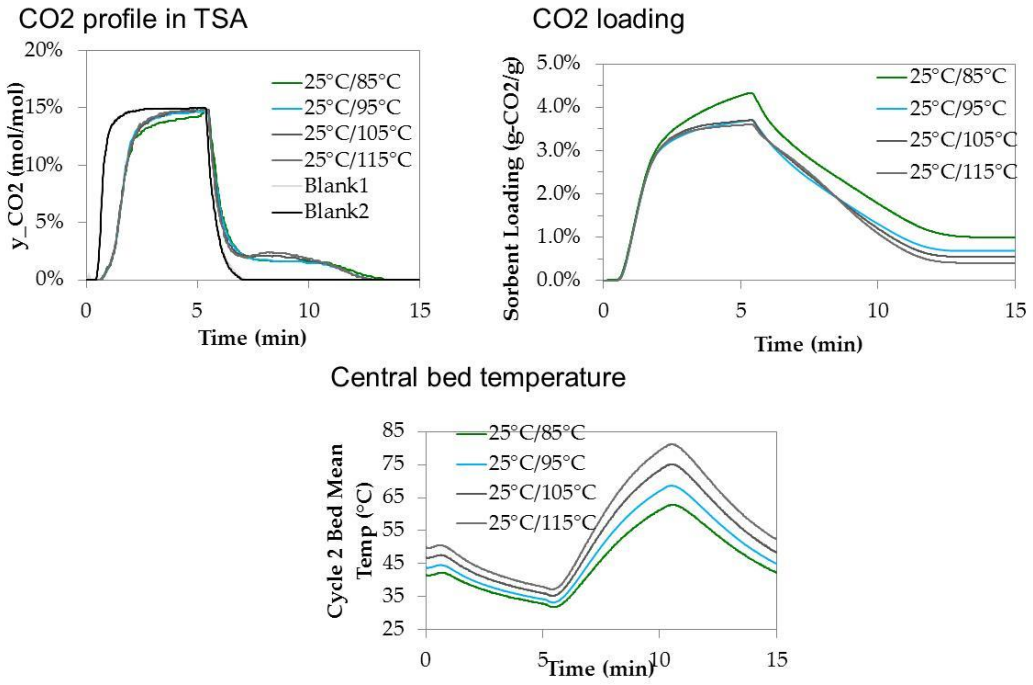

Figure 9. Adsorption testing results of structured bed module #61445-1-CO2-7 by increasing desorption temperature (tested in Jan. 4th week, 2013)

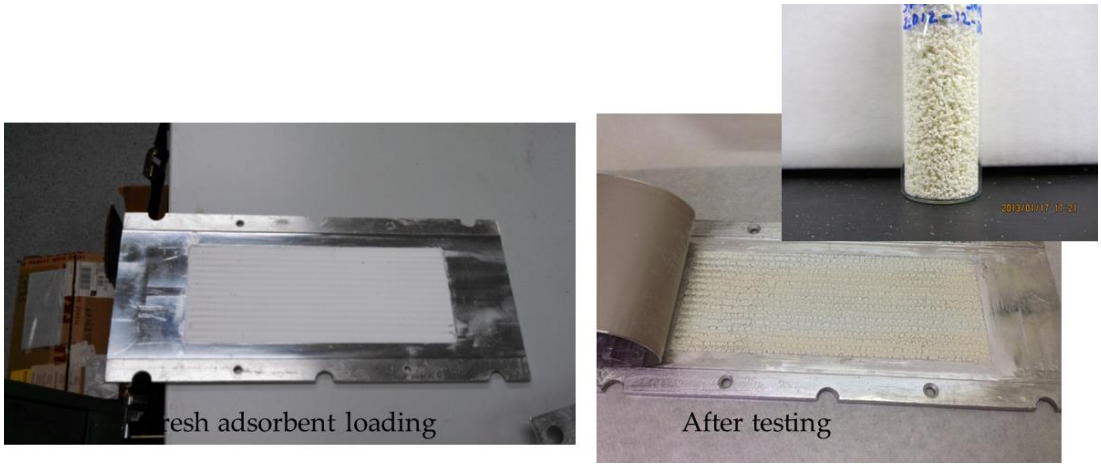

Figure 25. Examination of deactivated adsorbent from structured bed module #61445-1-CO2-7 by increasing desorption temperature

A fraction of the spent adsorbent unloaded from the above structured bed was sieved and loaded into the ½" OD reactor tube. The adsorption and regeneration cycles (Figure 26) were conducted at 45 ^{o}C. The resulting CO_2 loading was only 1 wt%. Thus, this adsorbent material was indeed de-activated.

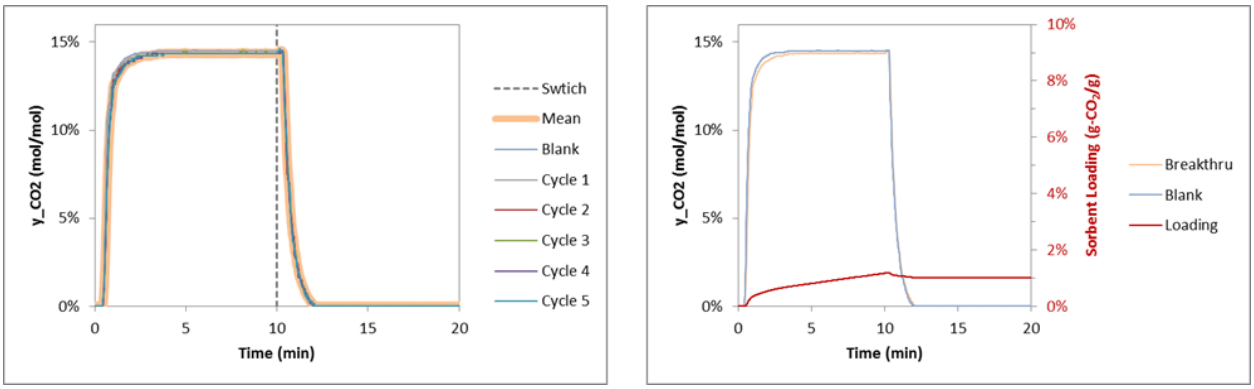

Figure 26. Adsorption testing of spent adsorbent particle from structured bed module #61445-1-CO2-7 at 45^{o}C (desorption by N^2 purge)

It was suspected that the silicone adhesive in RTV used to bond the porous metal sheet onto the Al frame may have had some detrimental effects on the adsorbent material. Thus, third structured bed was packaged without using RTV fluid. Instead, vacuum sealing tapes and Al duct tapes were used to seal the porous metal sheet on the Al frame (Figure 27). The average adsorbent loading was 2.5 g/each plate and total adsorbent loading was 17.5g.

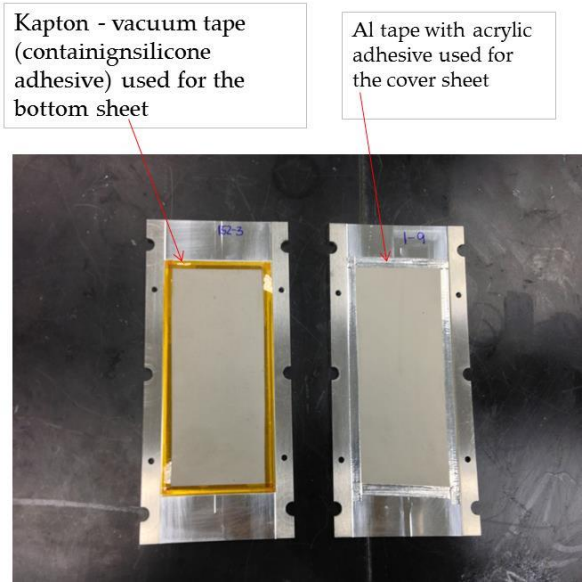

Figure 27. Adsorbent plates used for packaging of 3rd structured bed module (61445-3-CO2-7 plate)

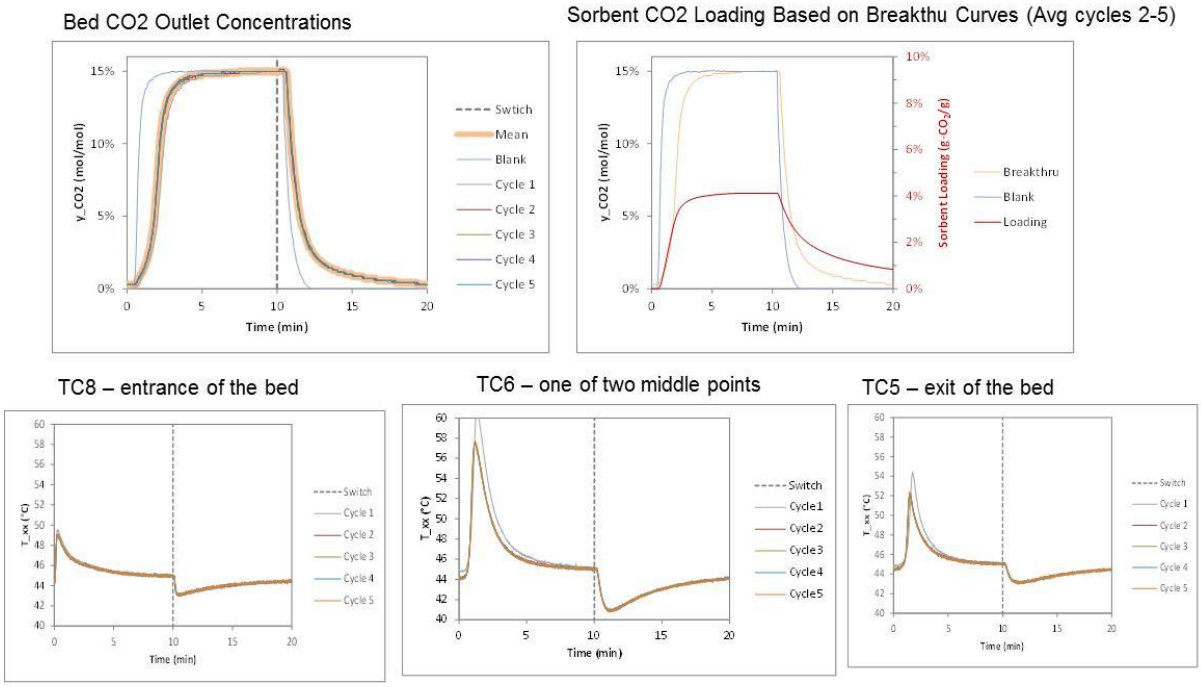

Figure 28. Adsorption/N_2 purge at a constant heat jacket temperature (45 ^{o}C) of 3rd structured bed (61445-3-CO2-7 plate)

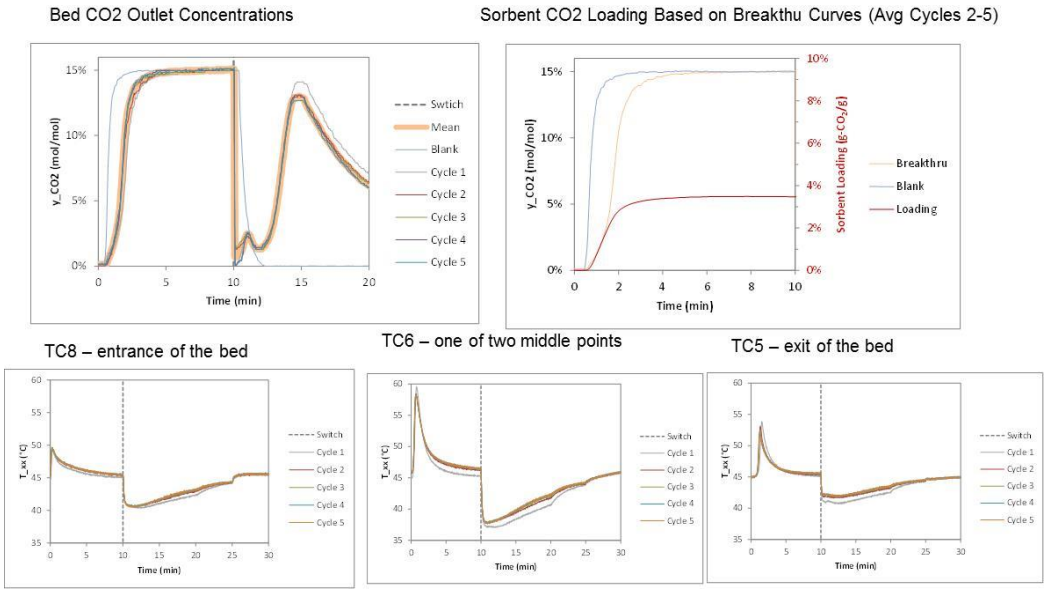

Figure 29. Adsorption/vacuum at a constant heat jacket temperature (45 ^{o}C) of 3rd structured bed (61445-3-CO2-7 plate)

Adsorption and desorption tests of the new structured bed were conducted by keeping the heat jacket temperature constant at 45 ^{o}C. As typical runs, desorption by N_2 gas purge was evaluated first (Figure 28). Pronounced effects due to heat of adsorption were observed. The temperature rise-up in the middle point of the bed was as high as 15 ^{o}C at the peak of adsorption. The degree of the temperature rise-up at the entrance and exit of the bed was less than that in the middle, which can be explained by thermal conduction. By contrast, the degree of the bed temperature variation during desorption was much smaller than that during adsorption. The difference indicates a slower desorption rate and/or in-complete desorption of adsorbed amounts. The resulting CO_2 loading was only 4.0 wt%.

Then, the same bed was tested with desorption by pulling vacuum. The adsorption, regeneration, and bed temperature profiles are plotted in Figure 30 for 5 consecutive cycles. The reactor pressure was switched between 17.8 and 1.8 psia (Figure 30), which corresponds to partial pressures of CO_2 of 2.7 psia at adsorption and 1.8 psia at desorption (assume 100% CO_2). The reactor pressure could be pressurized and de-pressurized in seconds. The pressure swing is much faster than the thermal swing. Significant temperature rise-up and drop-down from the baseline were observed during adsorption and desorption, which resulted from the heat of adsorption. The CO_2 working capacity of 3.5 wt.% was obtained. Given the small differential in partial pressure of CO_2 between adsorption and desorption, this working capacity is encouraging.

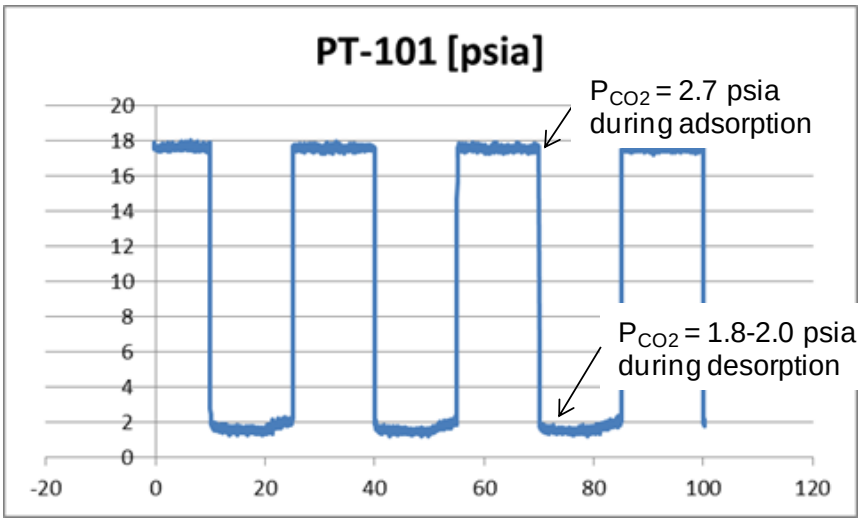

Figure 30. Reactor pressure profile during pressure-vacuum swing testing of 3rd structured bed (61445-3-CO2-7 plate)

It was speculated that the large temperature rise-up and drop-down in the middle of the structured bed during the vacuum swing operation may result from in-sufficient thermal conductivity between the adsorbent plates. Thus, 4th module was packaged using Al fins instead of the Al mesh as spacers between the adsorbent plates. The volume fraction of the solid in the Al fin is about 20%, which is four times of the solid fraction in the mesh (~ 5%). Thus, the thermal conductivity between the adsorbent plates is expected to be enhanced by four times. Table 4 lists the amounts of the adsorbent loading in the plates, and the total loading was 17.8g.

Table 4 Package of 4th structured bed module #61445-CO2-7 plate with original adsorbent powder (TRI-PE-MCM41)

Plate #	Adsorbent, g
60036-165-8B	2.02
60036-165-8A	2.61
60036-138-7	3.08
60036-167-1	2.41
60036-139-5	2.06
60036-152-1	2.74
61444-1-4	2.87
Total	17.79

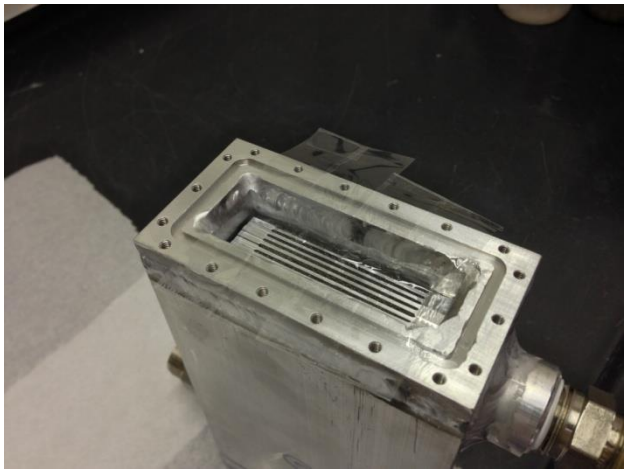

The 4th module was first evaluated for isothermal adsorption at 45 ^{o}C (Figure 31). The adsorption was conducted with feed gas of 15 % CO_2/N_2 at 50 % RH, while regeneration was conducted with dry N_2 gas purge. The CO_2 loading is estimated to be about 7 wt% in first cycle and stabilized to about 4 wt% in the subsequent runs. Using dry N_2 gas did not improve CO_2 loading. Then, an extended run sequence was executed with this adsorbent bed. Each testing cycle consisted of 10-min adsorption (14 % CO_2, 2.5 % O_2, balance N_2, humidified to 50 %) and 10-min dry N_2 purge. About 210 adsorption/regeneration cycles were done with a total time of about 70 hours. The adsorption breakthrough and bed temperature profiles at the beginning and end of the run look similar (Figure 32), which indicates no apparent adsorbent degradation or re-activation under these conditions.

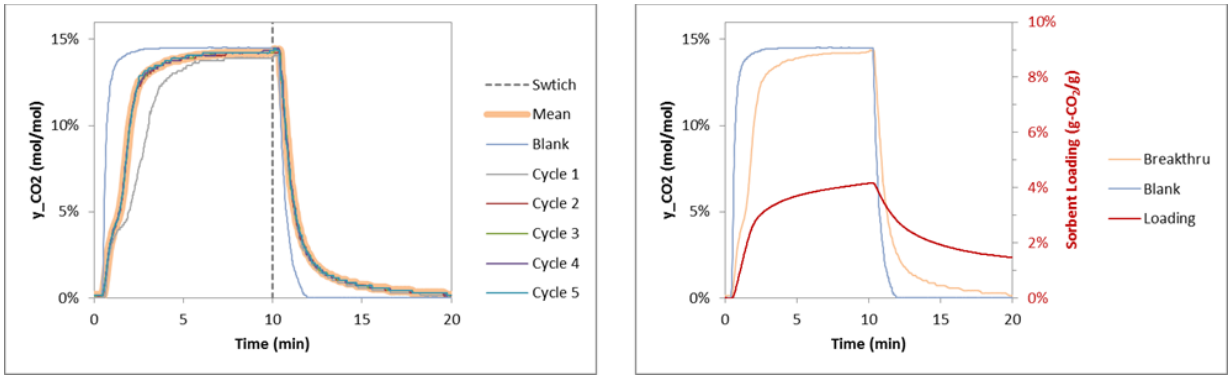

Figure 31. Initial adsorption testing results of 4th module#61445-CO2-7 (jacket temperature maintained at 45 °C for both adsorption and regeneration)

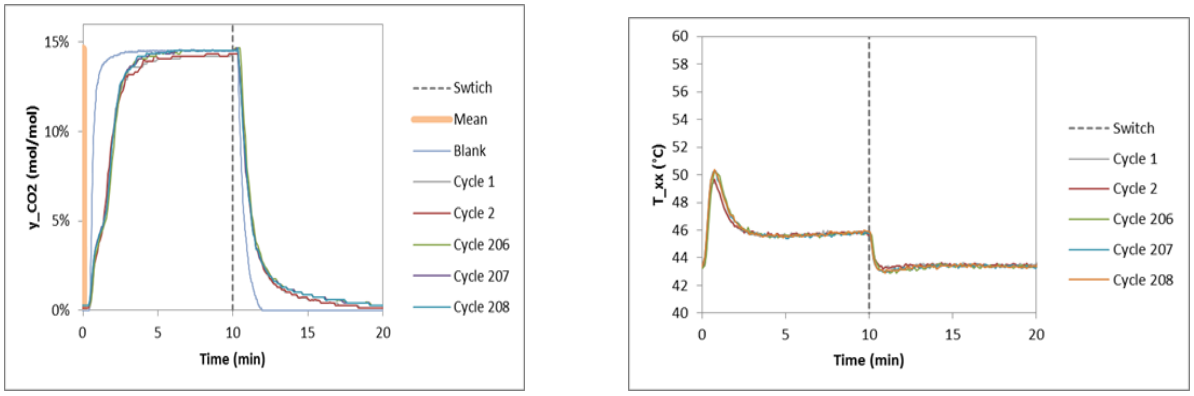

Figure 32. Extended adsorption testing run of 4th module#61445-CO2-7 (jacket temperature maintained at 45 °C for both adsorption and regeneration)

Since this adsorbent material is stable under ambient air conditions, re-activation of the adsorbent material by exposure to dry air was examined. No apparent changes were observed by exposing the adsorbent to stagnant air overnight (Figure 33). After 2-week storage in the dry air, the CO_2 loading was increased from 4 to 4.5 wt% (Figure 33). The testing results confirm the stability of the adsorbent material exposure to dry air at room temperature.

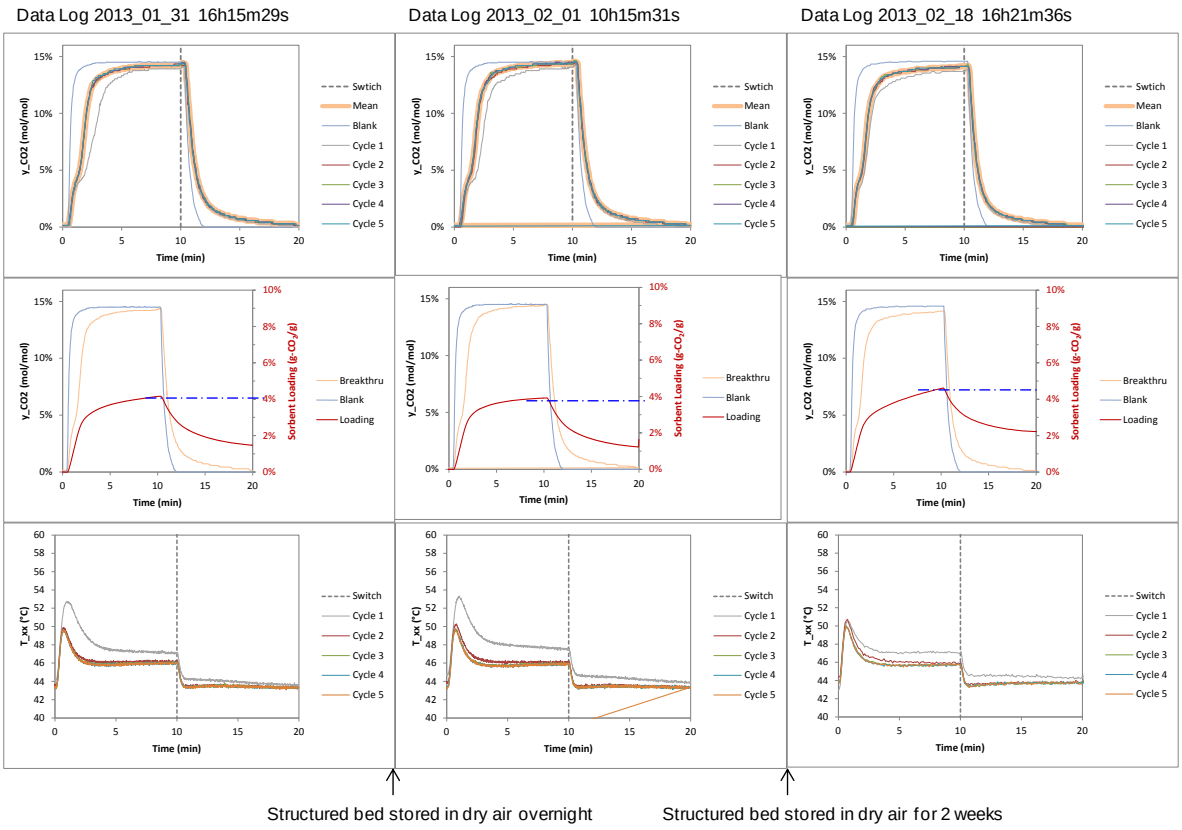

Figure 33. Impact of adsorbent storage in dry air on adsorption performances (4th module#61445-CO2-7, jacket temperature maintained at 45°C for both adsorption and regeneration)

The 4th module was tested with vacuum regeneration (Figure 34). The feed gas for adsorption consisted of 14.5 % CO_2, 2.5 % O_2, and 83 % N_2. The pressure during regeneration was only 0.5 psia, which is substantially less than the 1.8 psia pressure used previously. The reactor jacket temperature was maintained at 45°C by circulation of heat exchanging fluid. 20 cycles were performed. CO_2 loading was stabilized at about 3.2 wt%. The degree of temperature variation is much less than the previous run with 3rd module. This can be attributed to the enhanced thermal conductivity between the adsorbent plates. Because the Al fin was a dense material, the gas diffusion length in the channel was doubled compared to the Al mesh. The lower CO_2 loading may be caused by more channel diffusion resistance.

The combined temperature and pressure swing operation was tried to conduct adsorption at a lower temperature and desorption at a higher temperature under vacuum. The pressure swing between 16psia for adsorption and 0.5psia for desorption was rapid. The temperature swing was

a slower process because it takes time for the heat to be transported from the jacket into the bed. First set of the temperature swing tests (Figure 35) was conducted by flowing the hot fluid (95 ^{o}C) through the jacket for 5 min and the cold fluid (25 °C) for 5 min. CO_2 working capacity was stabilized at about 4.5 wt%. In second set of the temperature swing tests (Figure 36), the hot fluid temperature was the same but the cold flow temperature was reduced to 15^{o}C. In addition, the fluid was switched at a different time from the pressure. The fluid was switched from the hot to the cold in 2.5 min upon adsorption during 5-min adsorption process. The fluid was switched from the cold to the hot in 3.5min upon start of vacuum during 5-min regeneration. In this way, the CO_2 adsorption loading was increased to about 5.0 wt%. The third set of swing operation was conducted in a sequence same as used in the 2nd set of runs except that the cold fluid temperature was lowered to 5 ^{o}C and the hot fluid temperature was raised to 105 ^{o}C. The resulting CO_2 adsorption was about 5.5 wt%.

These extensive tests demonstrate that the CO_2 working capacity can be alternated by changing adsorption and regeneration conditions. However, the degree of the change is still below the initial adsorbent particle capacity.

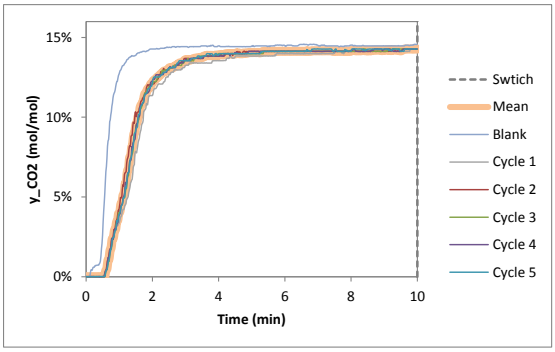

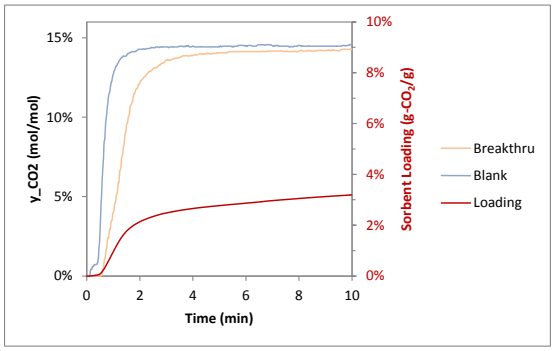

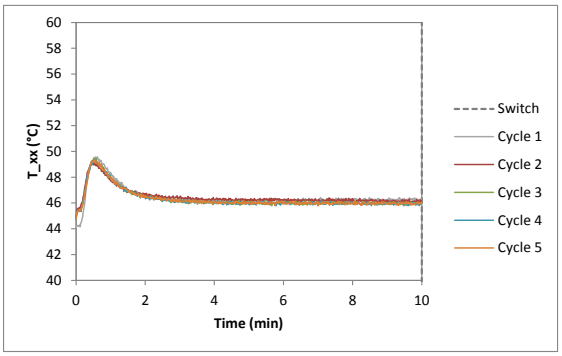

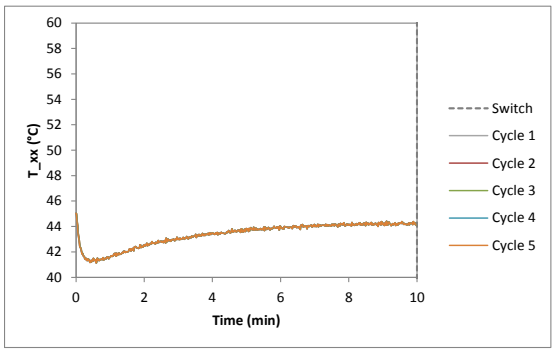

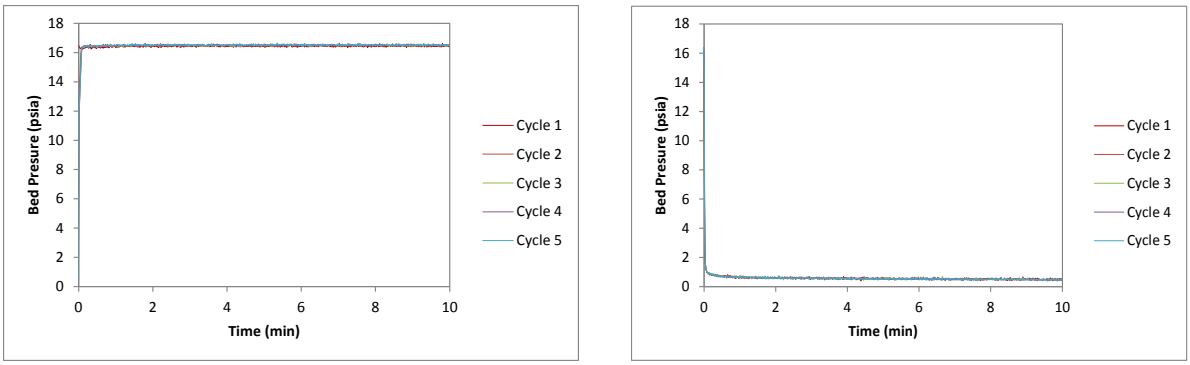

Figure 34. Vacuum swing adsorption tests of 4th module#61445-CO2-7, jacket temperature maintained at 45 ^{o}C for both adsorption and regeneration)

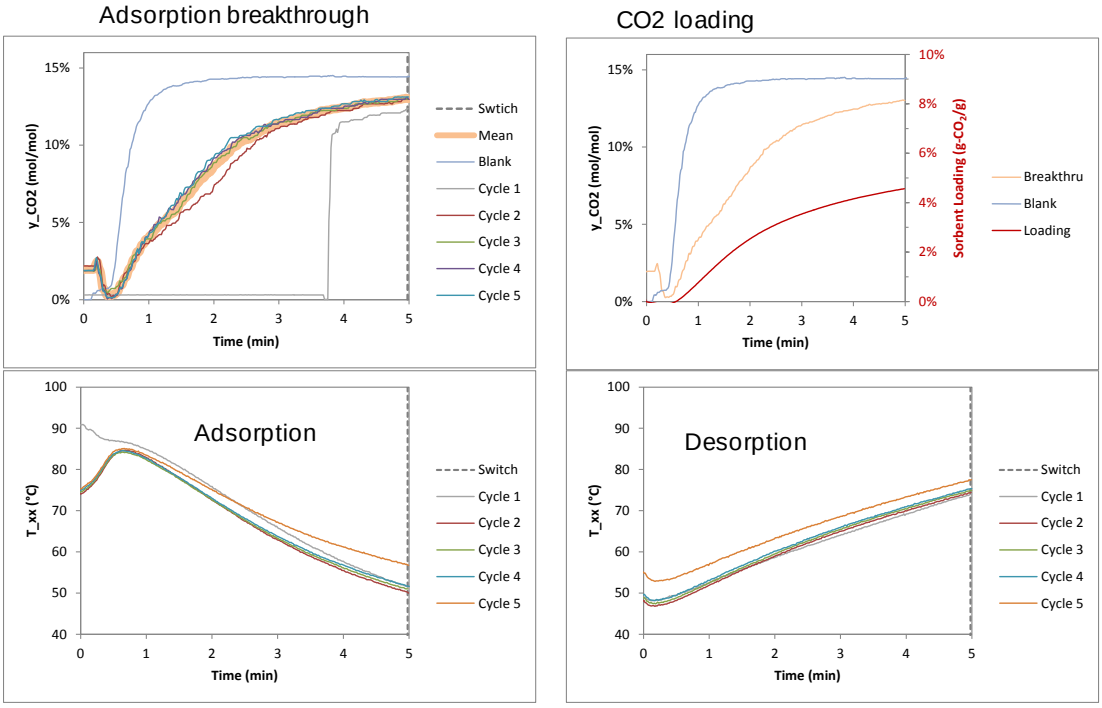

Figure 35. Combined temperature & vacuum swing tests of 4th module#61445-CO2-7 (pressure swing: 16psia ←→0.5 psia; heat exchanging fluid swing: 25 ^{o}C←→95 ^{o}C)

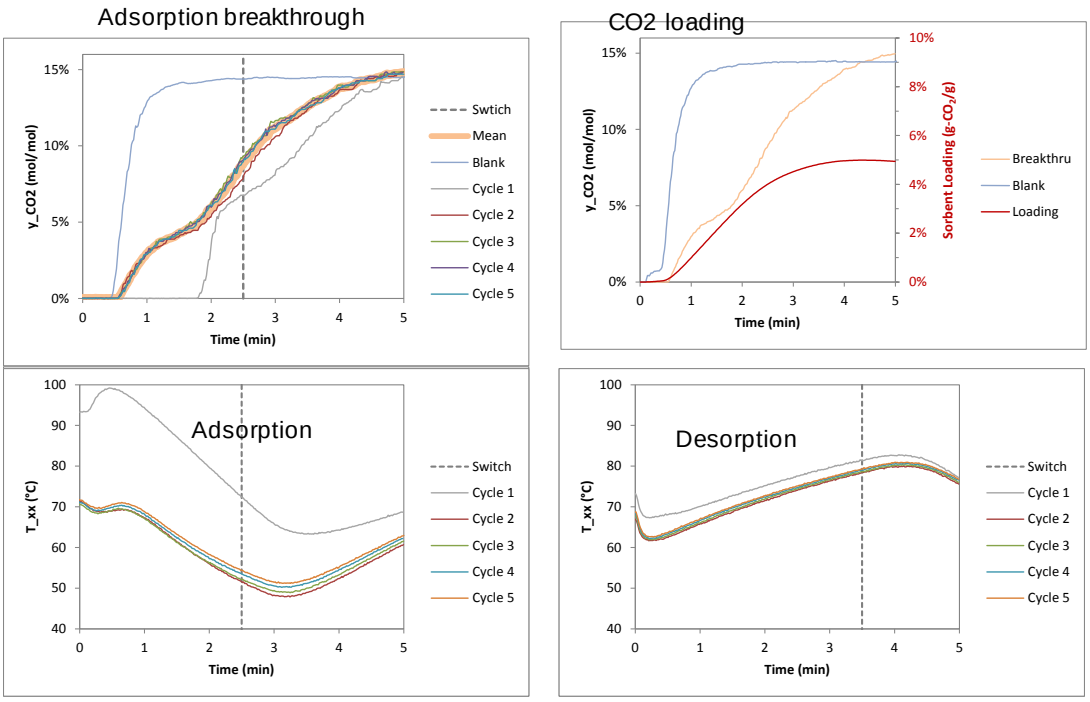

Figure 36. Combined temperature & vacuum swing tests of 4th module#61445-CO2-7 (pressure swing: 16psia ←→0.5 psia; heat exchanging fluid swing: 15 °C←→95 °C)

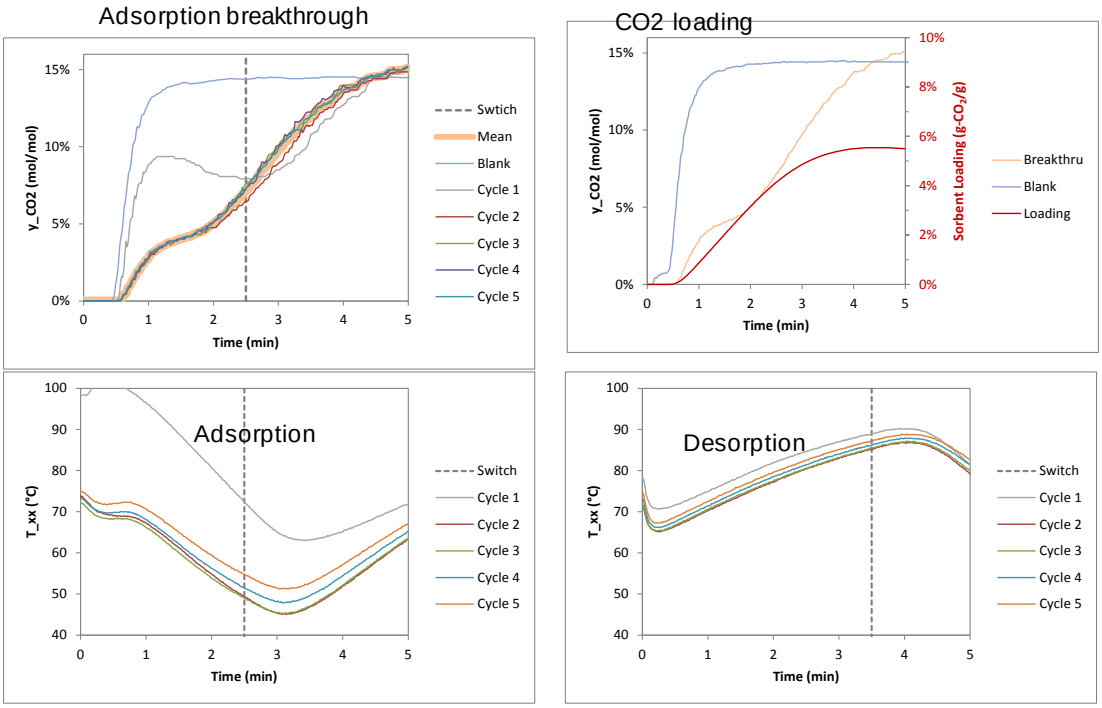

Figure 37. Combined temperature & vacuum swing tests of 4th module#61445-CO2-7 (pressure swing: 16psia ←→0.5 psia; heat exchanging fluid swing: 5 °C←→105 °C)

3.5 Testing of PEI-impregnated adsorbent in a structured bed

Meso-porous silica powder (SBA-15-PL) provided by University of Ottawa was impregnated with a PEI/iso-propanol solution at a weight ratio of PEI: Silica = 0.38:1.0. A certain amount of PEI was first dissolved in IPA completely. Then, the silica powder was added into the solution. This silica powder had fairly low packing density. Thus, a relatively large volume of the solution was needed to get the solid powder fully suspended. The IPA solvent was gradually vaporized from the suspension during stirring in fume food. The evaporation was stopped when the suspension was concentrated suitable to be loaded into the adsorbent plate. The adsorbent plates were packaged into the reactor cartridge. The cartridge was dried at room temperature and followed with drying at 120 ^{o}C under vacuum overnight. The drying temperature is much higher than 60 ^{o}C –the temperature reported in Prof. Sayari's publication. The rationale was to get the adsorbent stabilized for testing under various conditions. About 22g of the adsorbent was loaded. This was 5th structured bed module prepared in this project (Module #61445-5-CO2-7).

The bed was tested by adsorption/N_2 gas purge at 45 ^{o}C. The concentration and temperature profiles are plotted in Figure 38. The CO_2 loading was about 1 wt%, fairly low. As a result, there was little change in the bed temperature during the adsorption and desorption process. Then, extensive tests were performed with an attempt to rejuvenate the adsorbent. The results are summarized in Table 5. The CO_2 loading was consistently low, indicating this is not an active adsorbent. The CO_2 loading reported in the literature for this-type material was ranged from a few wt% to 10 wt%. The low CO_2 loading obtained in this project was likely due reaction and agglomeration of the PEI polymer at the high drying temperature, which reduced accessibility of the active sites by CO_2 molecules.

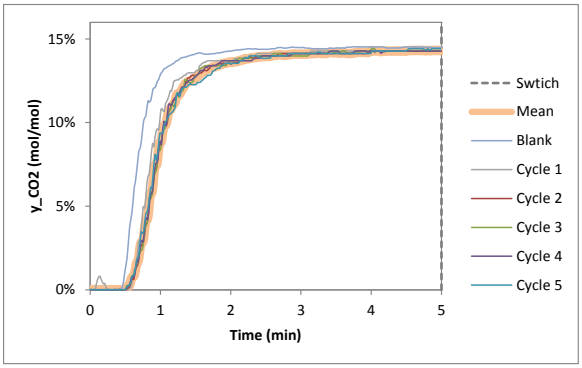

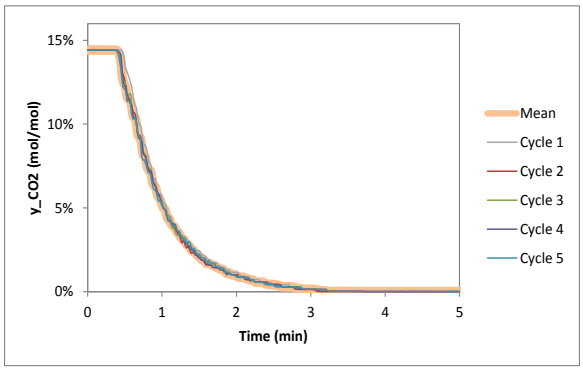

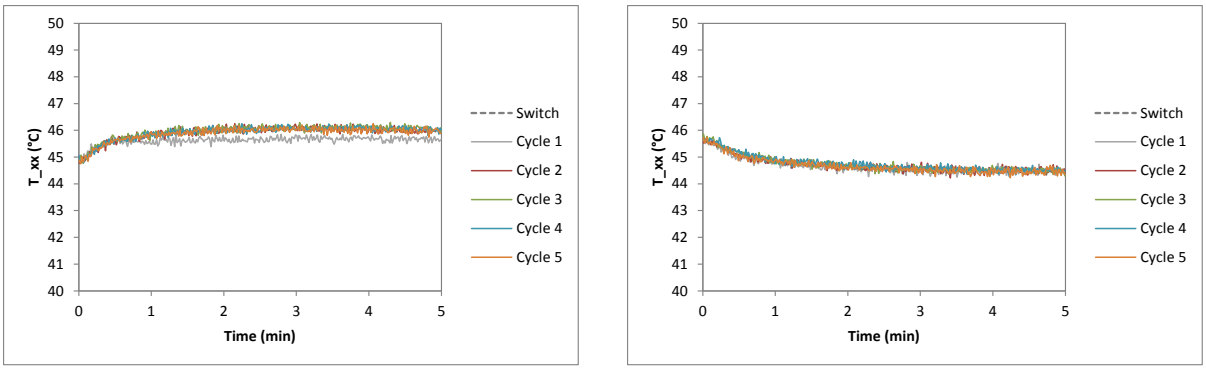

Figure 38. Isothermal adsorption tests of PEI-impregnated adsorbent material in structured bed (Module #61445-5-CO2-7; reactor jacket temperature at 45 °C)

Table 5. Testing results of the structured bed loaded with PEI- impregnated meso-porous silica (Module #61445-5-CO2-7)

Run#	Testing conditions	CO_2 working capacity
1	Isothermal Adsorption/N2-Purge at 45 °C	~ 1 wt%
2	Isothermal Adsorption/N2-Purge at 75 °C	~ 1 wt%
3	Isothermal Adsorption/N2-Purge at 95 °C	~ 0.9 wt%
4	Vacuum Swing Adsorption Test at 75 °C (15 psia → 0.5 psia)	~ 0.9 wt%
5	Combined Temperature and Vacuum Swing Adsorption Test Data (5 Cycles)	~ 1.5 wt%
6	Combined Temperature and Vacuum Swing Adsorption Test Data (Extended Cycles -27)	~ 1.5 wt%

IV. Process design (PNNL lead)

4.1 Theoretical analysis

Determining regeneration method and conditions is necessary to develop process designs. Due to low partial pressure of CO_2 in adsorption (0.15 bar for 15 % CO_2 in an atmospheric flue gas), the adsorbent has to be heated up to produce a CO_2 stream at atmospheric pressure. Regeneration was always conducted by reducing CO_2 partial pressure (either N_2 gas purge or pulling vacuum) in this work. Regenerating the adsorbent by heating up at atmospheric pressure is not demonstrated for the present adsorbent material. No literature report has been known for any other CO_2 adsorbent that can be regenerated by heating up in atmospheric pressure. The following thermodynamic analysis is conducted to determine relationship of the heat of adsorption with adsorption and regeneration conditions

Assume Langmuir adsorption equation

$$\theta = \frac{q}{q_0} = \frac{K \cdot p}{1 + K \cdot p}$$

Under adsorption conditions (T_{ad}, p_{ad})

$$\theta_{ad} = \frac{K \cdot p_{ad}}{1 + K \cdot p_{ad}}$$

$$\frac{1}{\theta_{ad}} = 1 + \frac{1}{K_{ad} \cdot p_{ad}}$$

$$K_{ad} = \frac{1}{p_{ad}} \cdot \frac{\theta_{ad}}{1 - \theta_{ad}}$$

Under desorption conditions (T_{des}, p_{des})

$$K_{des} = \frac{1}{p_{des}} \cdot \frac{\theta_{des}}{1 - \theta_{des}}$$

Adsorption equilibrium constant is related to heat of adsorption by classical thermodynamic equation

$$\frac{dLn(K)}{dT} = -\frac{Q}{RT^2} \qquad \text{i.e., } K = A \cdot Exp(\frac{Q}{RT})$$

$$\frac{K_{des}}{K_{des}} = EXP(\frac{Q}{R}(\frac{1}{T_{ad}} - \frac{1}{T_{des}}) = \frac{p_{des}}{p_{ad}} \cdot \frac{\theta_{ad}}{\theta_{des}} \cdot \frac{1-\theta_{des}}{1-\theta_{ad}}$$

$$Q = R \cdot \frac{T_{ad} \cdot T_{ad}}{T_{des} - T_{ad}} \cdot \ln[\frac{p_{des}}{p_{ad}} \cdot \frac{\theta_{ad}}{\theta_{des}} \cdot \frac{1-\theta_{des}}{1-\theta_{ad}}]$$

Relationship of heat of adsorption (Q) with regeneration temperature and adsorption working capacity is illustrated by the plots in Figure 39. For a given set of adsorption conditions, to release the CO_2 at 1.0 bar pressure, the required regeneration temperature decreases with increasing heat of adsorption. In other words, it is not possible to achieve low heat of adsorption and reduce the regeneration temperature at the same time. If the regeneration temperature is fixed, the heat of adsorption increases with working capacity. In other words, it is not possible to have an adsorbent having low heat of adsorption and provide high working capacity at the same time.

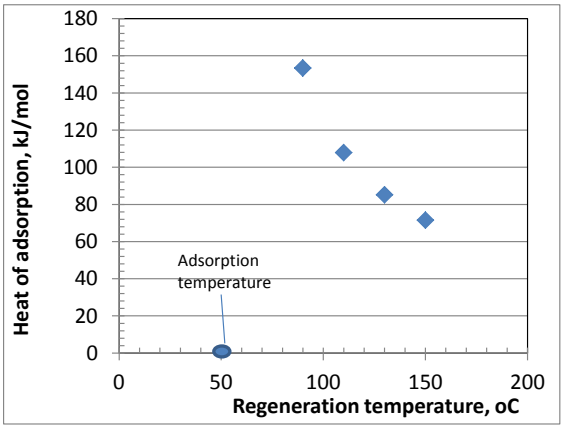

(a). Working capacity Δθ=0.8

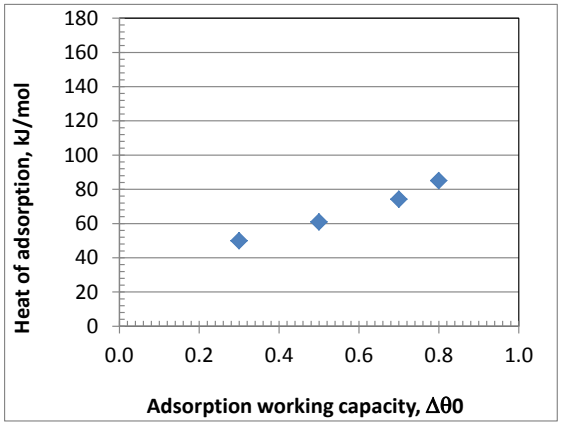

(b). Constant desorption temperature 130 ^{o}C)

Figure 39. Thermodynamic calculation of heat of adsorption at different working capacity and desorption temperature (constant adsorption conditions: 50 ^{o}C, θ_{ad}=0.9, p_{ad} = 0.15bar; desorption: p_{des} = 1.0 bar)

The heat of adsorption for the grafted adsorbent is deduced from the experimental data using the above Langmuir adsorption equation. From the Arrhenius plots (Figure 40), the heat of adsorption is estimated to be 10 - 20 kJ/mol based on CO_2 loading data measured at PNNL and University of Ottawa (UO). At such a low heat of adsorption, this adsorbent could not be regenerated by heating up at 1.0 bar pressure. The regeneration can only be done by reducing the pressure.

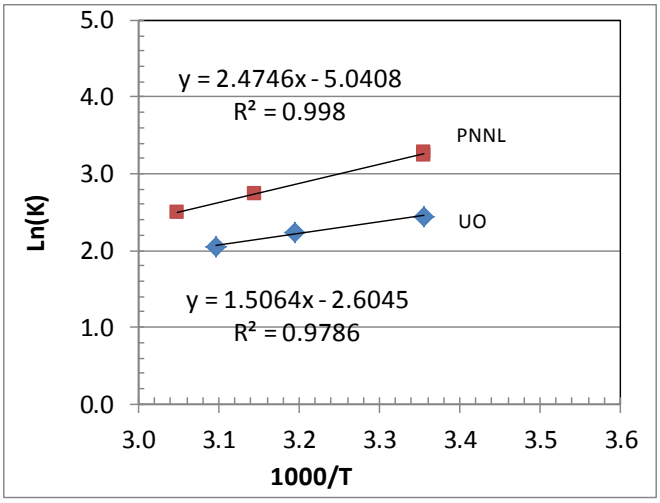

Figure 40. Arrhenius plots of adsorption equilibrium constants for the amine-grafted adsorbent

4.2. Preliminary CFD modeling

Supplemental funding was obtained from PNNL's Energy Conversion Initiative to conduct preliminary CFD modeling of the structured bed. The simulation was done by modifying the software developed previously for bead-packed beds and completed by end of September. With well-defined geometries of the structured bed, the dynamic temperature and concentration profiles can be generated with the CFD model simulation. Figures 41 and 42 show the CO_2 concentration and temperature profiles of a centerline section of the structured bed, respectively. Progressive movement of the adsorption front is illustrated with the concentration profiles at 20, 30, and 40 second from start of the adsorption. The temperature profiles in Figure 42 reveal presence of the high temperature region in the bed, which is caused by head of adsorption. As expected, the temperature becomes more uniform for the adsorbent plate closer to the heat exchange interface. The simulation results confirm the importance of effective thermal conduction of the adsorbent bed to the temperature uniformity of the bed. Due to its simple flow state (laminar flow) and well-defined bed structures, it is expected that the structured bed performance at large scales can be well simulated after the model parameters are validated with the small-scale experimental tests. However, the experimental validation of the model requires significant resources and was not planned in this phase of work.

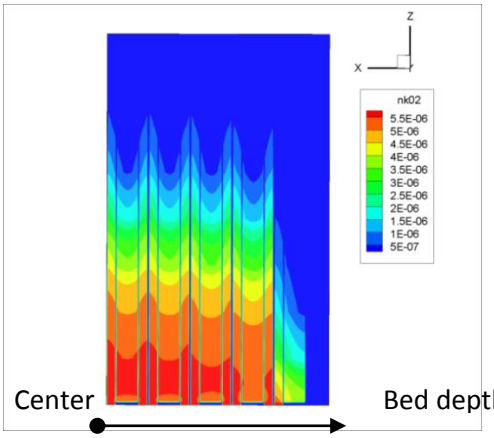

(a). t=20 sec

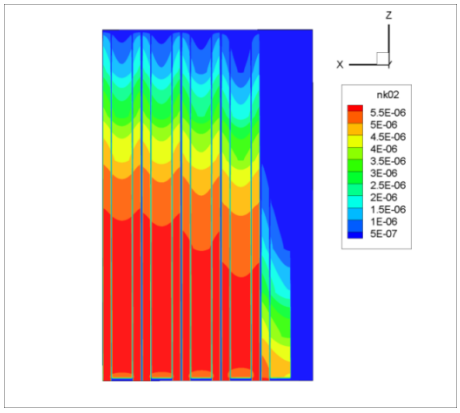

(b). t=30sec

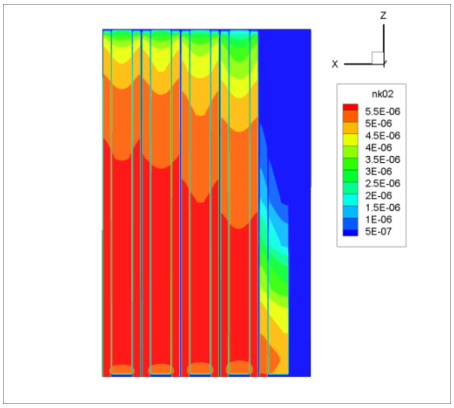

(c). t=40 sec

Figure 41. CO_2 concentrations (mol/cm^3) inside the flow channels of a structured bed (the centerpiece of the bed is cut along the bed height and half of it is shown)

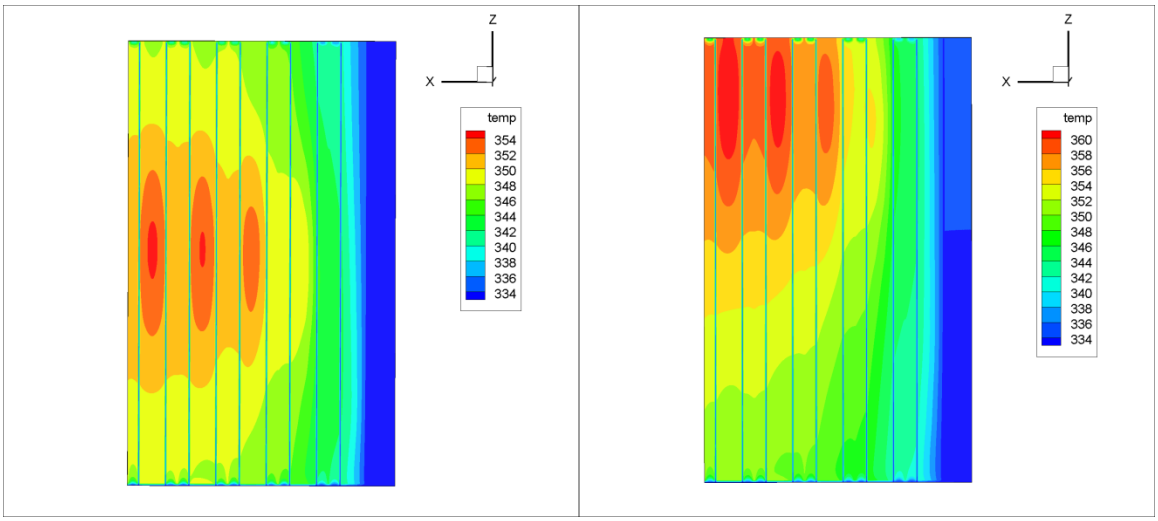

(a). t=20 sec (b). t=30sec

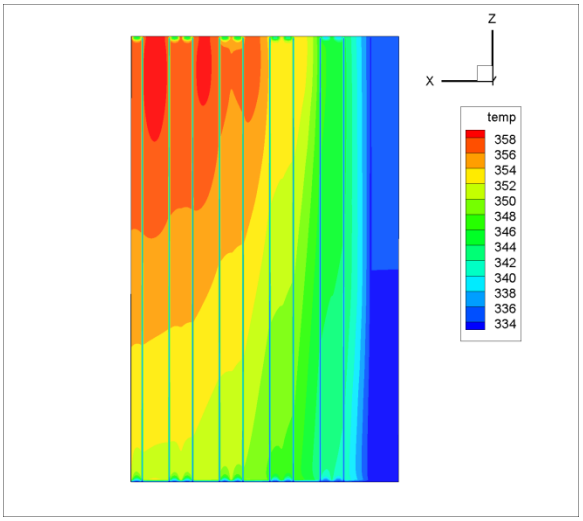

(c). t=40 sec

Figure 42. Temperature (K) distribution profiles inside the flow channels of a structured bed (the centerpiece of the bed is cut along the bed height and half of it is shown)

4.3 Process flow diagram and bed fabrication proposed

Based on the testing results and above theoretical analysis, a vacuum pressure swing adsorption process (Figure 43) and structured adsorption bed (Figure 44) are proposed for an industrial adsorption process. The saturated adsorbent is regenerated by pulling vacuum. Circulation water is used to transfer the heat between the adsorption to the desorption reactor. The water temperature is boosted by exchanging with the CO_2 product stream discharged from the vacuum pump after the adsorption column. Thus, the proposed process does not require any steam as compared to thermal-swing process used for the amine solvent scrubbing process.

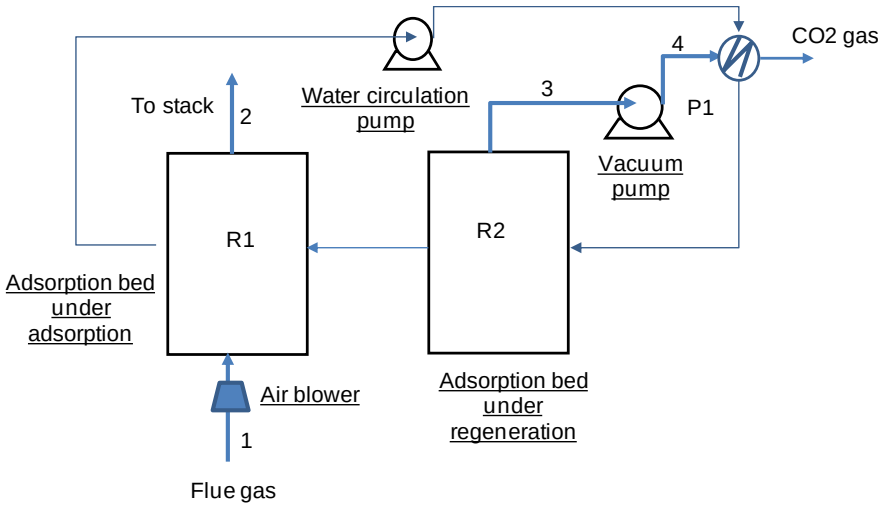

Figure 43. Simplified process flow diagram for an industrial CO_2 adsorption process

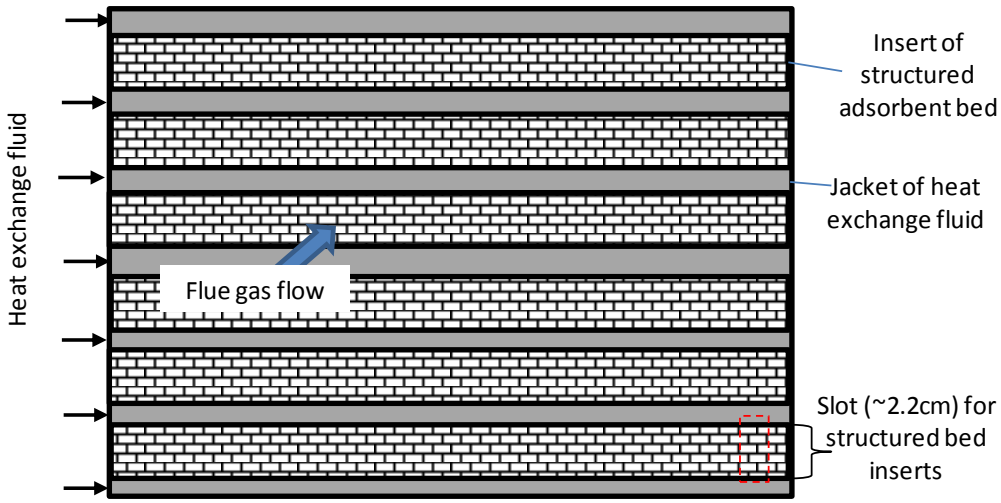

Figure 44. Schematic of structured adsorption bed

Given the large gas flow rate, nearly atmospheric pressure of the flue gas, and large sizes of the adsorbent bed, it is necessary to fabricate a structured adsorption bed to reduce the pressure drop. The large adsorption bed behaves like an adiabatic bed. Substantial temperature rise-up can be generated from heat of adsorption. Thus, it is also necessary to have embedded heat-exchanging conduits inside the structured bed. As a reference to the proposed adsorption bed, the plate-type selective catalytic reduction (SCR) reactor (Figure 45) is used in current industrial processes for reduction of flue gas NOx with ammonia.

Important process parameters for a 550 MWe-scale coal-fired power plant with adsorption CO_2 capture are listed in Table 6. With 3-min adsorption cycling time, the adsorbent required is about 846 ton and 1144 m^3 for a CO_2 working capacity of 3.5 wt%. If the working capacity is doubled to 7.0 wt% and the adsorbent packing density is increased from 0.75 to 1.0 g/cc, the required adsorbent is reduced to 423 ton and 423 m^3, which become very attractive.

Table 6 Important process parameters used for calculation of energy consumption for a 550 MWe-scale coal-fired power plant (NETL Case 10 Benchmark: 550 MWe net with CO_2 capture and subcritical steam cycle)

Adsorbent property	Low-capacity case	High-capacity case
Adsorbent packing density, g/cc	0.750	1.000
Heat of CO_2 adsorption, kJ/mol	50.0	50.0
Heat of H_2O adsorption, kJ/mol	0.0	0.0
CO_2 capacity, g/g_adsorbent	3.5%	7.0%
Stream 1 - flue gas composition, vol%		
CO_2	13.5%	13.5%
H_2O	15.4%	15.4%
O_2	2.4%	2.4%
N_2 + Ar	68.7%	68.7%
Total	100.0%	100.0%
Total flue gas flow rate, kg/h	3,213,261	3,213,261

Total flue gas rate, mol/s	30,959	30,959
Adsorption time, min	3.0	3.0
CO_2 capture	90%	90%
adsorbent needed, kg	846,346	423,173
adsorbent needed, m^3	1,128	423
Individual adsorbent plate		
CuNi metal sheet thickness, cm	0.005	0.005
Adsorbent layer thickness, cm	0.10	0.10
Volume fraction of Al insert	0.10	0.10
Overall thickness, cm	0.11	0.11
Package of adsorbent platen in each slot		
number of adsorbent plate	12	12
Spacing between adsorbent plate, cm	0.08	0.08
Fraction of Al spacer vol in channel	22%	22%
Hydraulic diameter, cm	0.16	0.16
Slot opening, cm	2.2	2.2
Volume fraction of components in each slot		
Fraction of adsorbent/slot	0.49	0.49
Fraction of channel flow/slot	0.312	0.312
Fraction of inert in plate/slot	0.11	0.11
Fraction of spacer solid/slot	0.088	0.088
Structured bed/total reactor, vol/vol	0.846	0.846
Total reactor volume, m^3	2,717	1,019

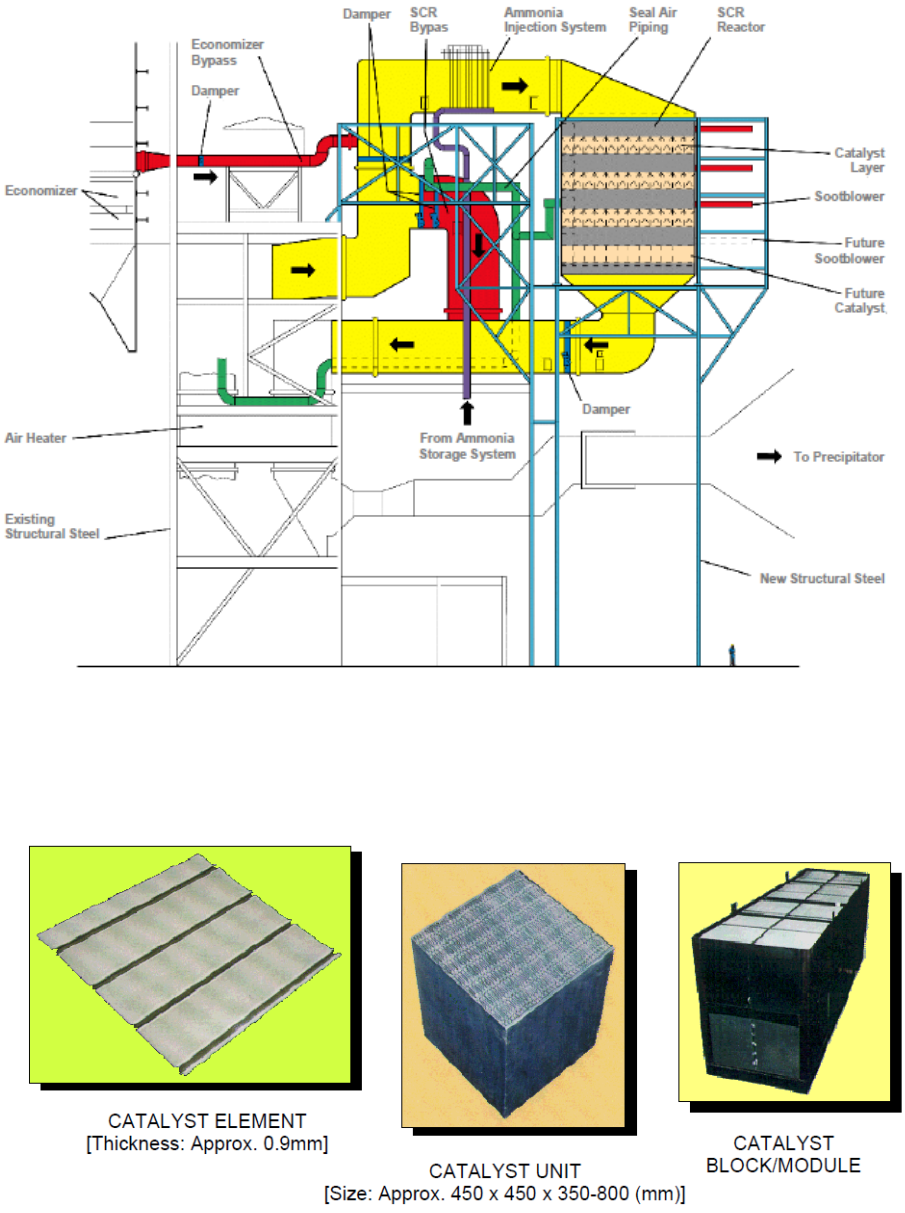

Figure 45. Plate-type catalytic reactor (Hitachi Catalytic Plate SCR – 675 MW Coal Fired Boiler)

A reactor system (Figure 46) consisting of 28 pods (or units) in three layers (16+8+4) is conceived to do rapid switching between adsorption and desorption in large-scale. Switching between adsorption and desorption at 3 minute intervals is realized by rotating rings on the front

and rear of the pods that use hydraulic actuated flexible seals to supply or block flue gas and the vacuum pumps. Initially the vacuum pumps will exhaust to the stack to maintain high CO_2 content in the compressed CO_2 gas.

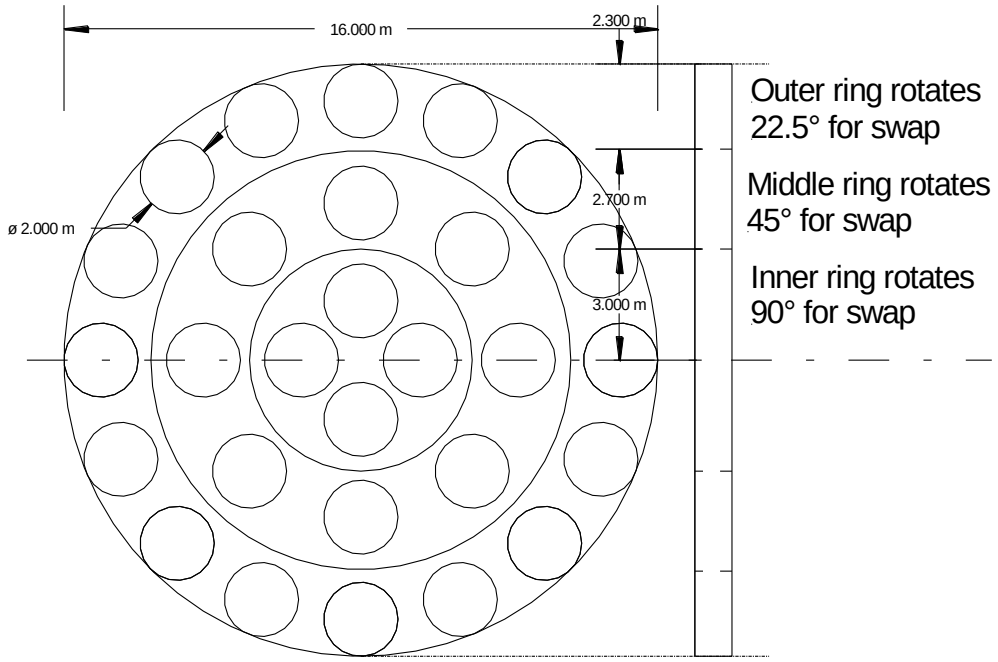

Figure 46. End view of layout for a rapid adsorption/regeneration switch reactor system consists of 28 Pods

4.4. Process efficiency and economics analysis

The 550 MW coal-fired power plant with CO_2 capture by amine solvent scrubbing from DOE/NETL report is used as the baseline for process economics analysis of the proposed structured bed system. The material and energy balances for the CO_2 capture process need to be integrated with the overall plant. Compared to the amine scrubbing process, major changes in the plant block diagram (Figure 47) with the adsorption process are (i) the CO_2 capture section, (ii) low-pressure gas turbine, and (iii) cooling water system. CO_2 capture unit is installed after the limestone, wet flue gas desulfurization. ISO – site conditions for plant are 59°F and 60% RH. Sub-critical steam cycle - single reheat16.5 MPa/566C/566C (2400 psig/1050°F/1050°F) is used for electricity generation.

Four process modules (Figure 48) are simulated with APEN Plus, including the adsorption section, steam cycle, cooling water, and CO_2 compression. The simulation results are displayed in Figures 49-52 for respective modules. The energy balances for the adsorption process are compared to the amine scrubbing process in Table 7.

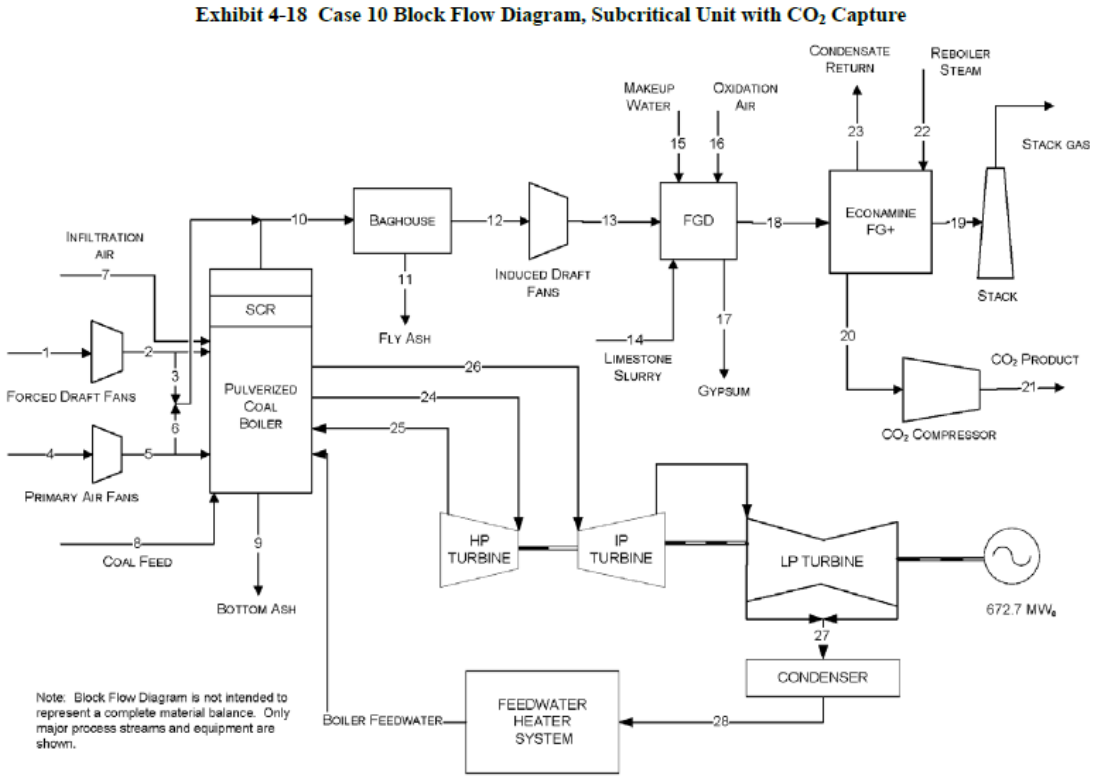

Figure 47. Process block diagrams of 550 MWe coal-fired power plant with CO_2 capture by amine scrubbing (DOE/NETL-2010/1397)

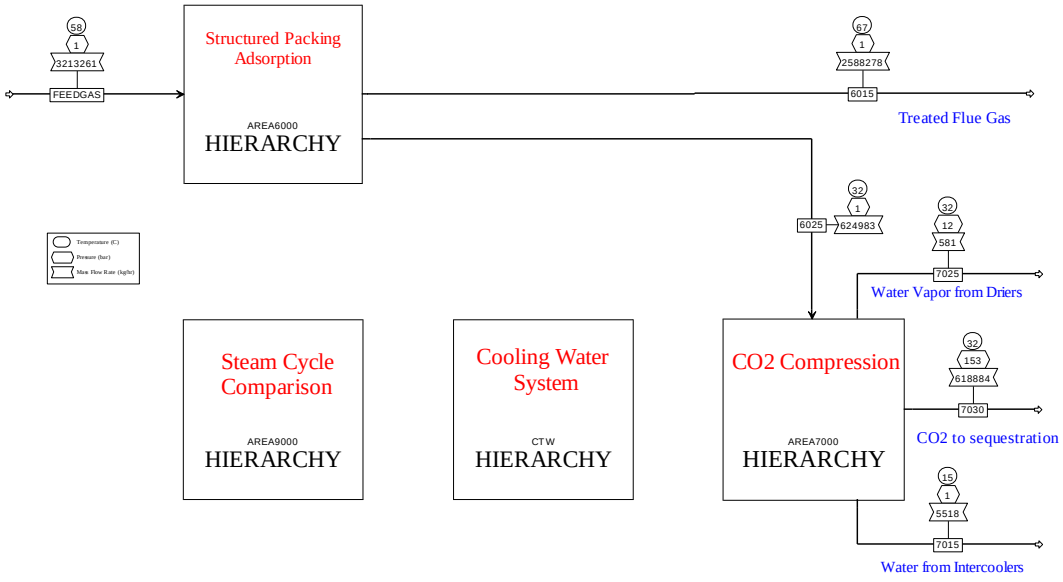

Figure 48. Aspen Simulation modules used

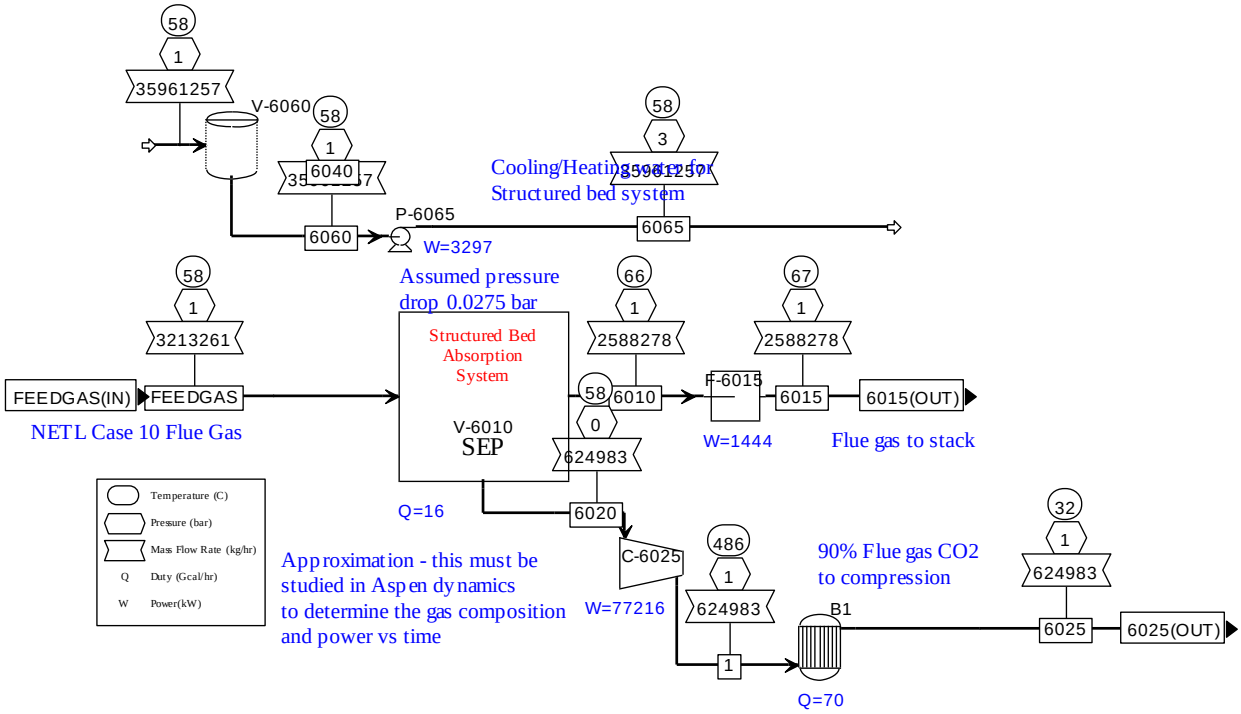

Figure 49. Process flow diagram of structured bed adsorption section

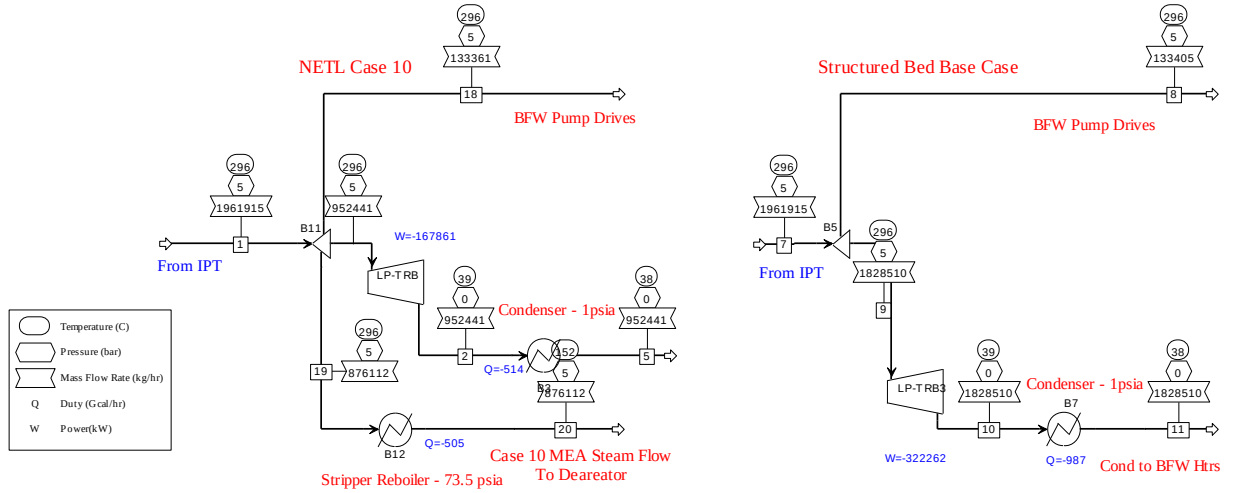

Figure 50. Comparison of steam cycles in NETL Case10 and in structured bed adsorption system

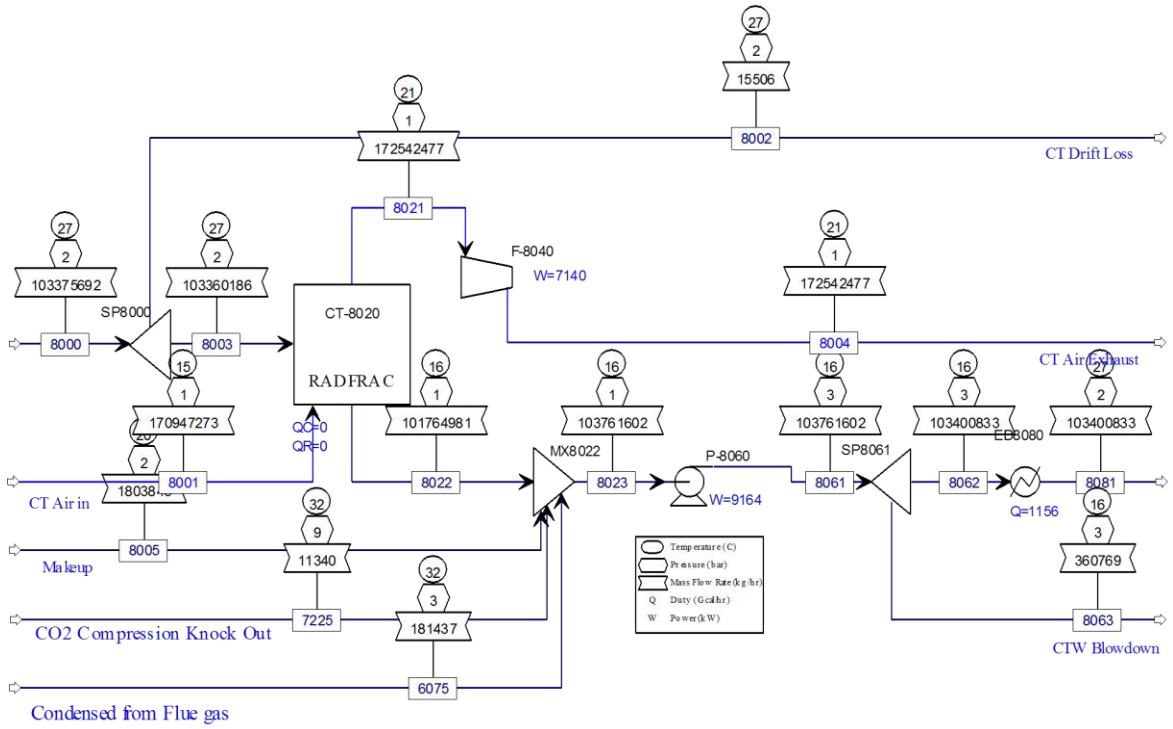

Figure 51. Process flow diagram of cooling water system

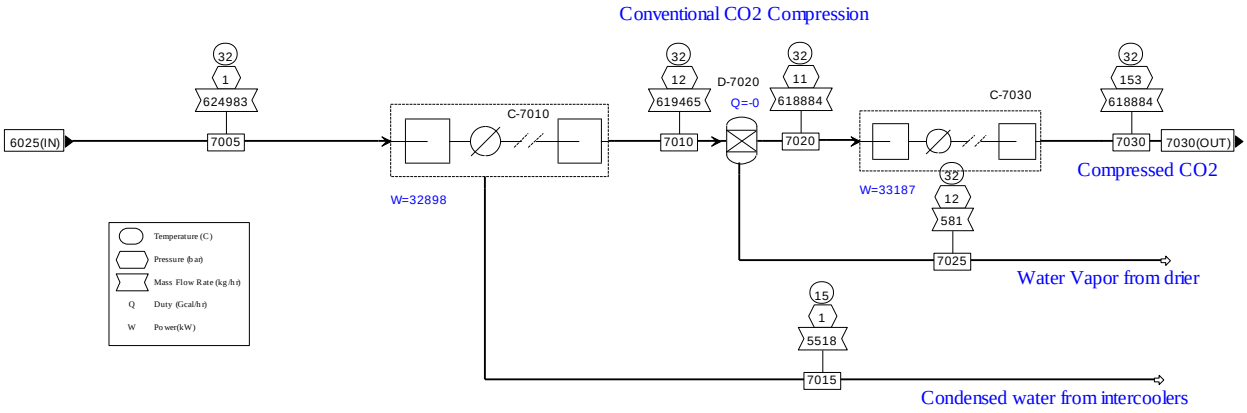

Figure 52. Process flow diagram of CO_2 compression system.

The key assumptions used in the simulation are as follows:

- No water is absorbed or desorbed from adsorbent during operation
- Absorbers are cooled with circulating water with a max 10°C rise
- Desorbers are cooled with the same circulating water at the same rate – thus there is no net input or output of heat assumed
- 90% CO_2; 1% N_2, Ar, H_2O; 5% O_2 of the flue gas appears in the desorbed gas
- The pressure drop across the device in flow conditions is 0.4 psi
- 4 kPa is assumed for desorption

Table 7. Comparison of energy balances of structured adsorption bed to amine absorption process (unit in kW, on the basis of the same amount of coal burnt)

	NETL Case 10	Structured Bed
Total Steam Turbine power	672,700	827,101
Auxiliary Load Summary		
Coal Handling and Conveying	540	540
Pulverizers	4,180	4,180
Sorbent Handling	1,370	1,370
Ash Handling	800	800
Primary Air Fans	1,960	1,960
Forced Draft Fans	2,500	2,500
Induced Draft Fans	12,080	12,080
SCR	70	70
Baghouse	100	100
Wet FGD	4,470	4,470
Econamine FG Plus Auxiliaries	22,400	
Structured Bed Auxiliaries		8,741
CO_2 Compression	48,790 (66,085)	126,006

Miscellaneous Balance of Plant	2,000	2,000
Steam Turbine Auxiliaries	400	400
Condensate Pumps	700	1,462
Circulating Water Pumps	11,190	23,377
Ground Water Pumps	1,020	2,131
Cooling Tower Fans	5,820	6,159
Transformer Losses	2,350	2,889
Total Auxiliaries	122,740 (140,035)	201,235
Net Power	549,960 (532,665)	625,866

The major saving with the adsorption process over the amine scrubbing process is low-pressure steam. Since no steam is needed for the pressure swing adsorption, 154,401 kW additional power output is produced from the LP turbine from burning same amount of coal. The major energy consumption to operate the adsorption process results from the vacuum pumps that remove the adsorbed CO_2 at 4 kPa and compress it to 1.0 bar. The energy consumption for subsequent CO_2 compression from 1 bar to the sequestration pressure is the same for the two processes. 8,741 kW of miscellaneous power consumption is assumed for the adsorption process, such as switching between adsorption and regeneration. Since a larger volume of circulating water is used for the adsorption process, the water circulation pump power consumption is higher for the adsorption process than for the amine scrubbing process.

As a net result, 13.8% more electricity power is produced from the plant with the adsorption CO_2 capture than with the amine capture process. In other words, compared to the plant without any CO_2 capture process, the energy penalty for the adsorption process is 24.3 % versus 33.5 % for the amine scrubbing. It should be noted that CO_2 compression power consumption of 48,790 kW presented in NETL's case appears to be very low. Using the simulation method same as used for the adsorption process here resulted in 66,085kW. For consistency, the original NETL number is used for comparison. If this number is corrected, 17.5 % higher power output is produced with the adsorption capture process.

The capital costs are made by referring to the related equipment in the industry. For 3.5% CO_2 working capacity, 28 reactor units are assumed for alternating adsorption and regeneration operation. These identical, small reactor units are proposed so that they may be mass produced at low costs and the standard unit also reduces the installation cost. Two valves are needed for each

reactor unit to turn the feed flue on/off and switch the exit gas between the stack outlet and vacuum outlet. No such large-scale vacuum pumps are known in industrial uses today. Technically, they are doable. These axial flow high compression ratio compressors similar to the compressors used for jet aircraft may be used for the vacuum pumping. The 4 kPa vacuum is equivalent to altitude of 67,000 ft. By contrast, U2 spy plane cruises at 90,000 ft and commercial aircraft Boeing 737 is certified to 41,000 ft. In conclusion, suitable compressors are not off the shelf but within current manufacturing capability. $10million/each cost is assumed. The resulting total capital cost is 195 million $. If the working capacity is enhanced to 7.0 wt%, the capital cost is reduced to about 160 million $.

The capital cost normalized by the power output is $312/KW and $256/KW for the 3.5 % and 7.0 % working capacity, respectively. They are much less than $792~950/kW for the amine scrubbing system.

The variable operation cost is dominated by the electricity consumption to drive the adsorption separation process. The structured bed cost is estimated to be $50 per Kg of the adsorbent material with the adsorbent powder material cost of $20/kg. As long as the adsorbent has reasonable lifetime, the adsorbent cost is minor.

Table 8. Estimated capital cost of the adsorption capture system (in $K)

Equipment	Unit cost	Installation factor	3.5 wt% working capacity		7.0 wt% working capacity	
			Number	Capital cost	Number	Capital cost
Reactor vessel	$1,000	2.0	28	$56,000	14	$28,000
Valves	$100	2.5	56	$14,000	28	$7,000
Water pump	$100	2.5	1	$250	1	$250
Vacuum pump	$10,000	2.5	4	$100,000	4	$100,000
Gas compressor	$10,000	2.5	1	$25,100	1	$25,000
				$195,350		$160,250

Table 9. Estimated operation cost of the adsorption capture system (5 year adsorbent lifetime assumed)

	Unit	3.5 % capacity	7.0 % capacity	3.5 % capacity	7.0 % capacity
Adsorbent	$/kg	Inventory, kg	Inventory, kg	Million $/Y	Million $/Y
	50	846,346	423,173	$8.5	$4.2
Electricity	cent/kwh	Consumption, kW	Consumption, kW		
	6.68	201,235	201,235	$107.5	$107.5
total				$116.0	$111.8

Acknowledgement

The author would like to thank Dr. Richard Zheng for all the adsorption tests, Mr. Nathan Canfield and Jirgal Mansurov for package of structured beds, Mark Bearden for process economics analysis, and David Reactor for CFD modeling.

References

1. Cost and Performance Baseline for Fossil Energy Plants Volume 1: Bituminous Coal and Natural Gas to Electricity Revision 2, November 2010; DOE/NETL-2010/1397
2. Isato Morita, Toru Ogasahara, Howard N. Franklin, “Recent Experience With Hitachi Plate Type Scr Catalyst” Presented ToThe Institute of Clean Air Companies Forum ’02, February 12-13.

APPENDIX

SUPPLEMENTARY REPORT

To be communicated

The following are a list of points to be addressed in the supplementary report, which I captured from today's meeting.

1. Put up a table to summarize all the testing results of the amine-grafted adsorbent in the structured bed concisely, which include critical conditions and working capacity.

2. Add comparison of footprints of the adsorption system to the amine scrubbing system
3. Put up a concise and critical summary of

    i. what we knew at the beginning of the project and what we anticipated to achieve through the project work;
    ii. what we actually achieved through this project, what we know and we do not know now.
    iii. define the performance criteria of an ideal adsorption system (a breakthrough CO_2 capture technology), propose the targets and approaches for the follow-on work, such as adsorbent stability, working capacity enhancement, and moisture impacts.

4. Further check those major assumptions used to make the cost estimate and energy efficiency calculation, identified risk factors and un-resolved issues related to commercialization, such as vacuum pumps and valves.